CHAPTER 6

IMPEDANCE SPECTROSCOPY STUDIES OF MG30 COMPLEXES

6.1 Introduction

The most significant study concerning polymer electrolytes is electrical conductivity. Many researchers such as Singh *et al.* (1998), Baskaran *et al.* (2004), Marzantowicz *et al.* (2006) and Austin Suthanthiraraj *et al.* (2009) have been studying the electrical conduction in polymer electrolytes intensively to understand the charge transport mechanism in the polymer electrolytes. The study of dielectric relaxation in polymer electrolytes is also a powerful approach for obtaining information about the characteristics of ionic and molecular interactions. The dielectric constant plays a fundamental role which shows the ability of a polymer material to dissolve salts because it is sensitive to the motion of charged species and dipoles of polymer electrolytes [Badr and Sheha, 2011].

In this chapter, an effort has been made to study the electrical conductivity and the dielectric properties of MG30 based polymer electrolyte at room and elevated temperatures. Results on the impedance studies of three polymer electrolyte systems: single salt MG30–$LiCF_3SO_3$, double–salt MG30–$LiCF_3SO_3$–$LiN(CF_3SO_2)_2$ and plasticized MG30–$LiCF_3SO_3$–PEG200 systems will be presented.

6.2 Conductivity studies of MG30–$LiCF_3SO_3$ films

Figure 6.1 shows typical Cole–Cole plots for stainless steel/MG30–$LiCF_3SO_3$/ stainless steel sandwiched structures with different amounts of $LiCF_3SO_3$ at 298 K. Typical plot consists of a high frequency semicircle followed by a low frequency straight line. It can be seen that Figures 6.1 (a) and (d) show a semicircle shape whereas the plots in Figures 6.1 (b) and (c) consist of a semicircle and spike implying double layer capacitance (Austin Suthanthiraj and Kumara Vadivel, 2011b).

The semicircle in the high frequency side of the plot is due to the bulk conductivity, which can be represented by parallel combination of bulk resistance and bulk capacitance of the polymer electrolytes. In Figures 6.1 (c) and (d), the Cole–Cole plot shows the appearance of a low frequency spike portion which leads to a conclusion that the current carriers are ions and hence the total conductivity is mainly the result of ion conduction.

The bulk resistance, R_b can be obtained from the intercept of the low frequency side of the semicircle with the real impedance axis. If the material consists of a pure capacitance, the complex impedance plot must show a straight line parallel to imaginary axis but the double layer at the blocking stainless steel electrode causes the inclination. This inclination indicates that capacitance is changing with frequency and it is due to electrode polarization [Jacob *et al.* 1997]. This inclination is also due to surface roughness [Song *et al.*, 2000]. From Figure 6.1, it has been found that with the increase of $LiCF_3SO_3$ concentration, the R_b value decreases and hence the conductivity increases.

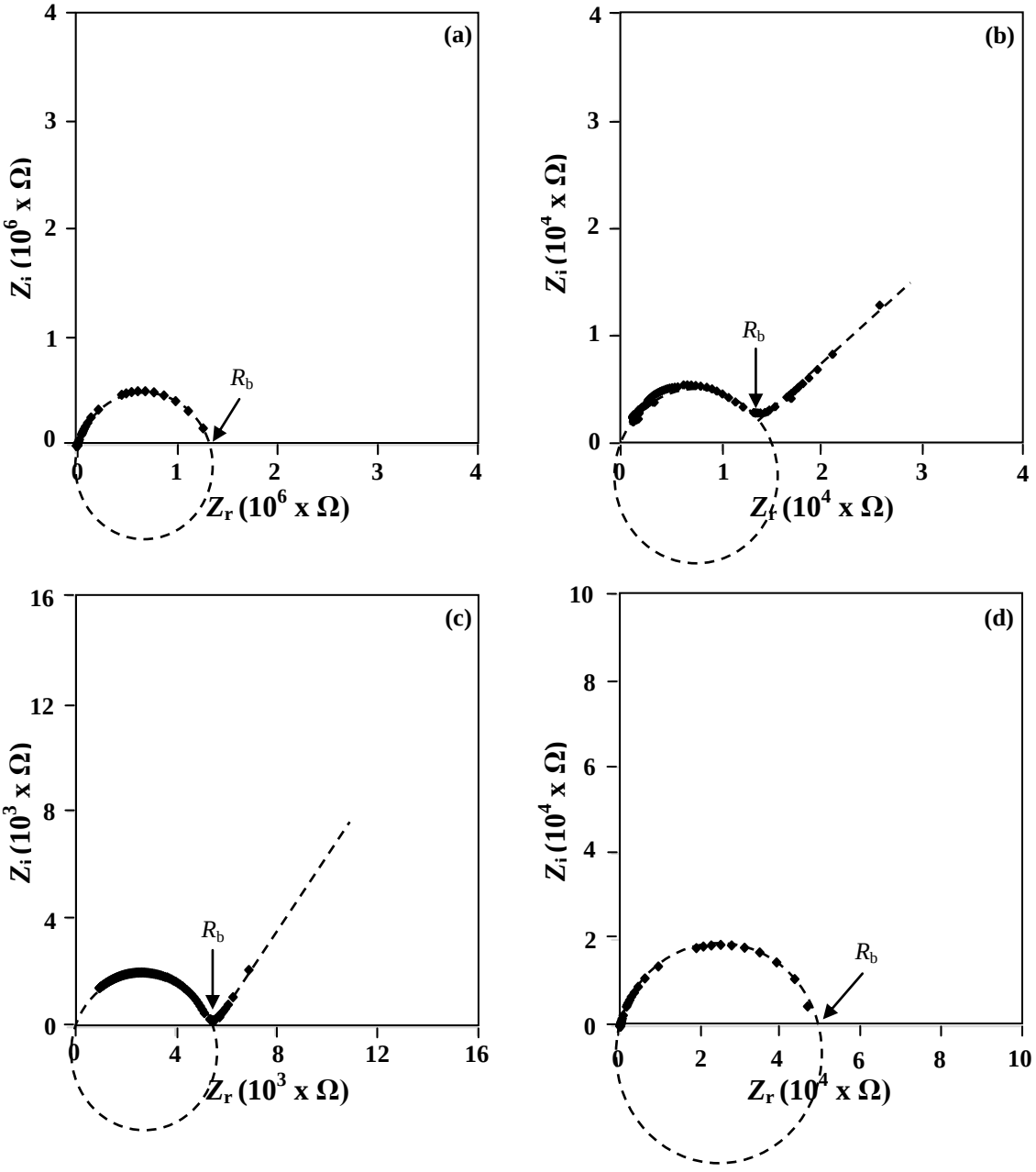

Figure 6.1 Cole–Cole plots of (a) MG10L, (b) MG20L, (c) MG30L and (e) MG40L at 298 K

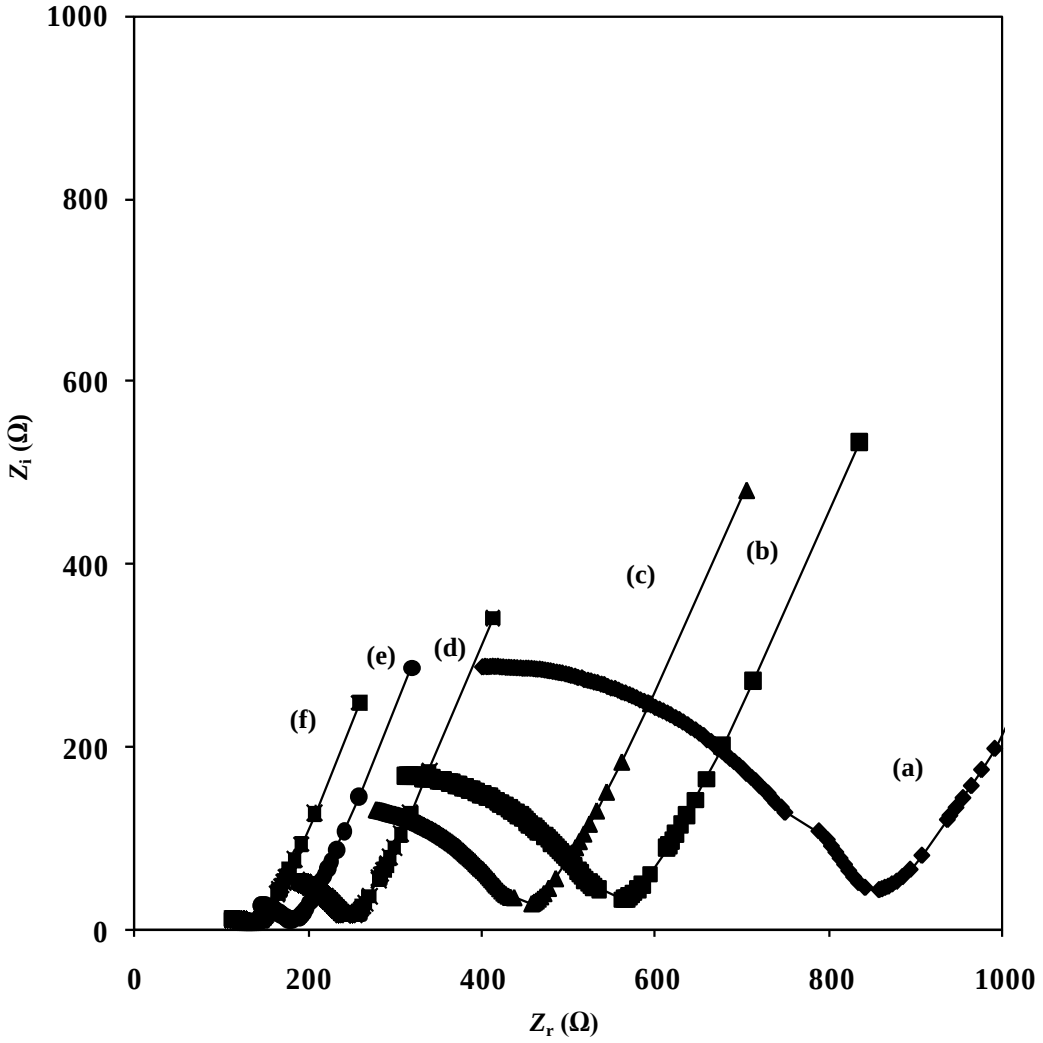

Figure 6.2 Cole–Cole plots for MG30L sample at different temperatures (a) 296 K, (b) 298 K, (c) 303 K, (d) 313 K, (e) 323 K and (f) 333 K

The Cole–Cole plots for MG30L for different temperatures are shown in Figure 6.2. It has also been found that the bulk resistance decreases with increasing temperature. The decrease in resistance of polymer electrolyte can be due to the enhancement in mobility with temperature [Malathi *et al.* 2010].

Figure 6.3 depicts the effect of amount of $LiCF_3SO_3$ on the ambient ionic conductivity values. It is shown that the conductivity of pure MG30 film is low, which is about 2.6×10^{-11} S cm^{-1} at room temperature. The ionic conductivity increased gradually until 1.69×10^{-6} S cm^{-1} when 30 wt. % $LiCF_3SO_3$ was added. Beyond the

amount of 30 wt. % $LiCF_3SO_3$ salt, the conductivity decreased. Figure 6.1 (c) represents the Cole–Cole plot of the highest conducting sample in the MG30–$LiCF_3SO_3$ salted system. The salt added to the sample provides Li^+ ions for the conduction of charge. The conductivity exhibited is 1.69×10^{-6} S cm^{-1} at 298 K and the conductivity decreased above that composition.

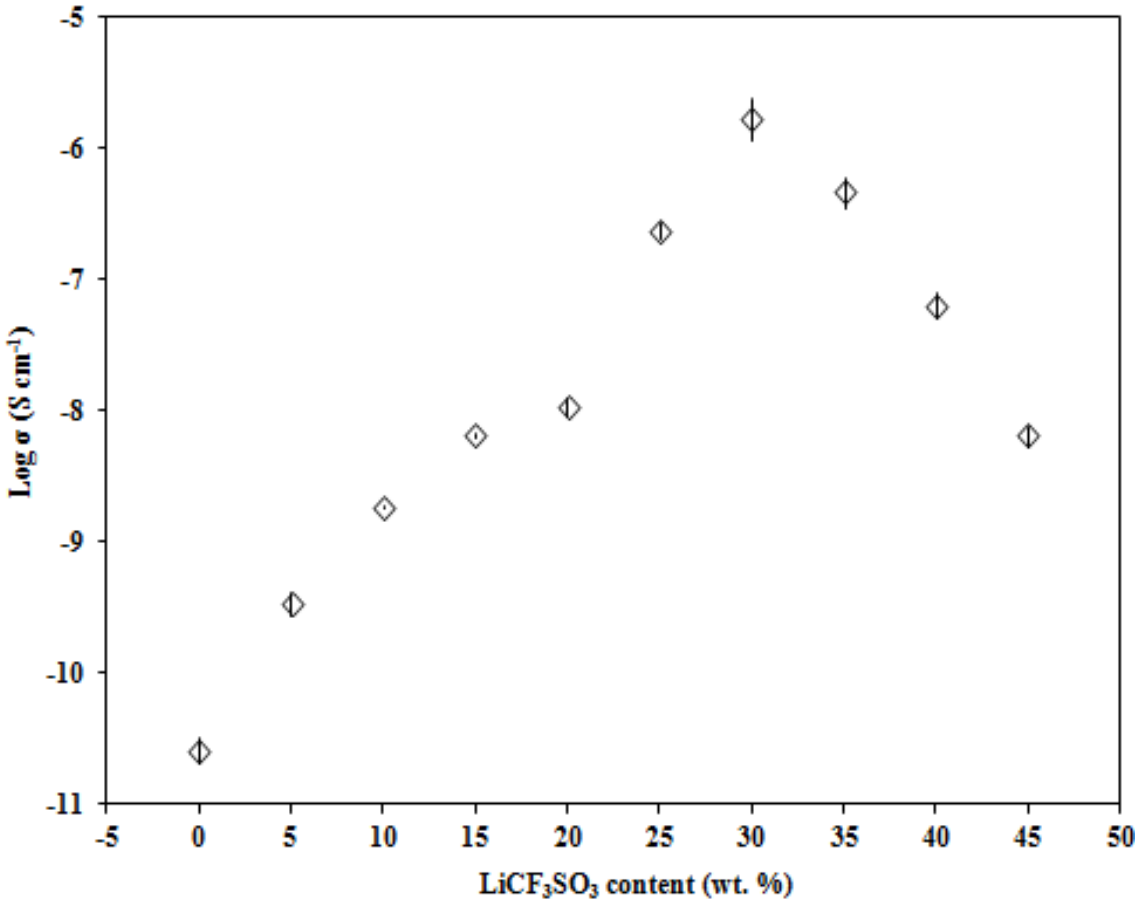

Figure 6.3 Effect of the amount of $LiCF_3SO_3$ on the conductivity of MG30 films at 298 K

Ionic conductivity, σ can be expressed as

$$\sigma = \sum_i n_i q_i \mu_i \qquad (6.1)$$

where n is carrier concentration, q is charge and μ is carrier mobility. Therefore, the increase by four orders of magnitude in the room temperature conductivity value from that of the pure polymer can be attributed to the increase in number of mobile ions

provided by the salt. Mobility of ions at this salt concentration is assumed constant at room temperature.

Plots of log σ vs 1000/T for MG30 containing different amounts of $LiCF_3SO_3$ are shown in Figure 6.4. The change in conductivity of the electrolyte for the MG30–$LiCF_3SO_3$ system from 298 K to 333 K is shown below.

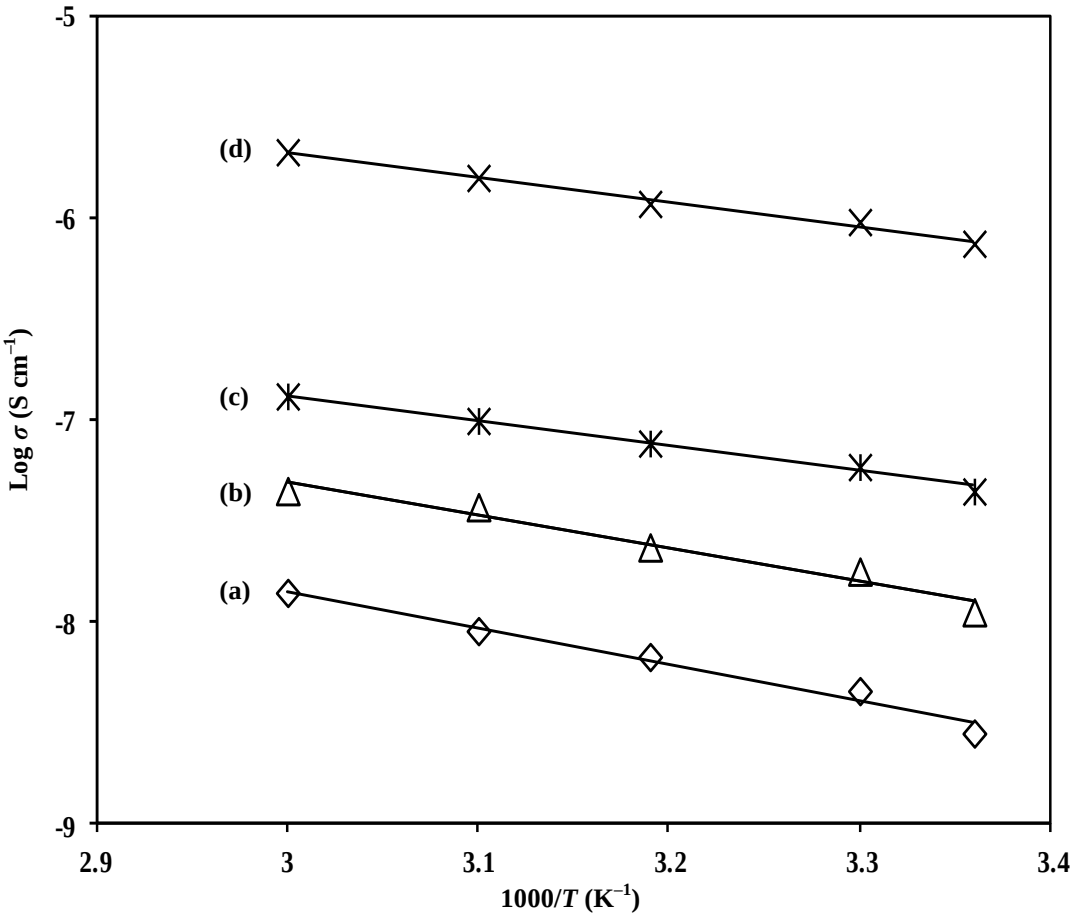

Figure 6.4 Temperature–dependent conductivity plots of (a) MG10L, (b) MG20L, (c) MG30L and (d) MG40L

Using linear regression method, the regression value, R^2 for every plot is close to unity indicating that σ versus T relationship is Arrhenius. The Arrhenius equation is shown below

$$\sigma = \sigma_0 \exp\left(-\frac{E_a}{kT}\right) \qquad (6.2)$$

where σ_0 is the pre–exponential factor, E_a is the activation energy, k is the Boltzmann constant and T is the absolute temperature in Kelvin.

Figure 6.5 shows the activation energy for $LiCF_3SO_3$ salted systems at 298 K. It can be concluded that the system with 30 wt. % $LiCF_3SO_3$ composition requires the least minimum energy to begin charge or lithium ion transfer, and it has the highest ionic conductivity. The activation energy, linear regression values and ionic conductivity are listed in Table 6.1.

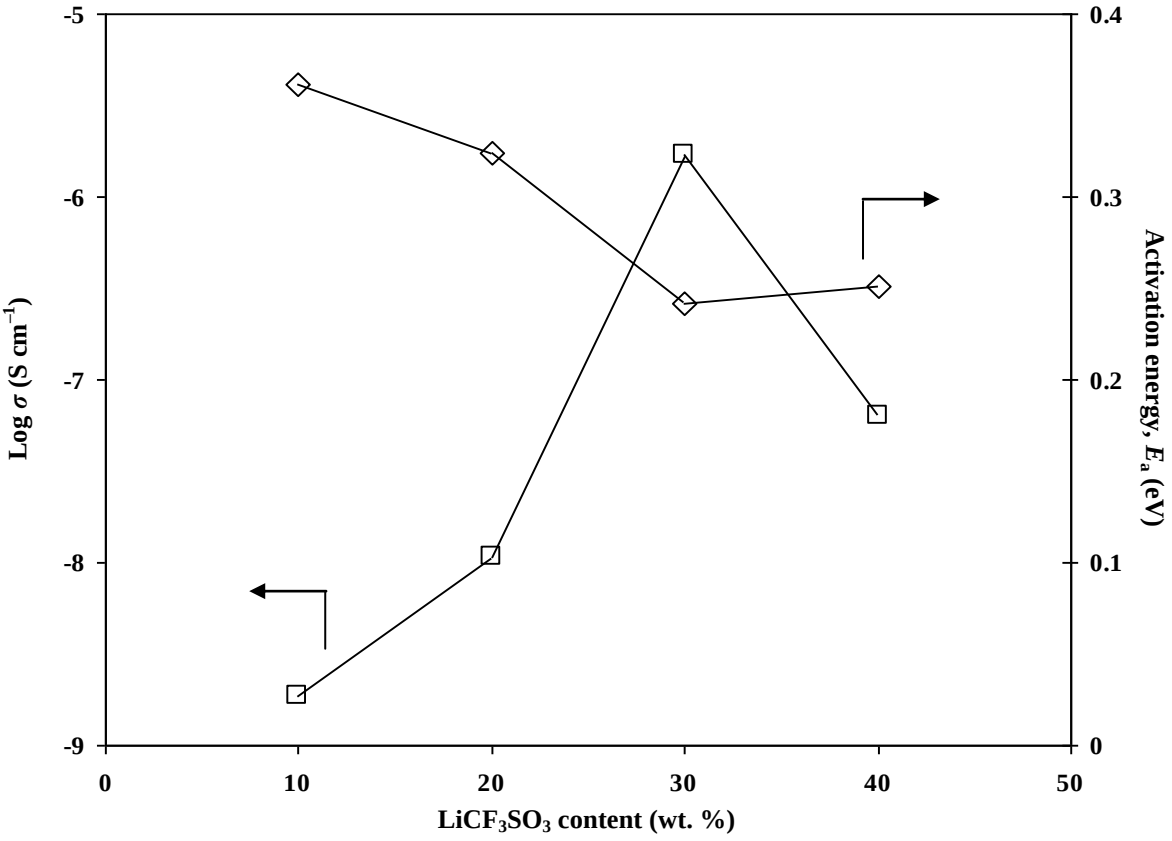

Figure 6.5 Log σ and activation energy of MG30–$LiCF_3SO_3$ polymer electrolyte system

Table 6.1: Conductivity parameters of the MG30–$LiCF_3SO_3$ polymer electrolytes

Designation	MG30:$LiCF_3SO_3$ (wt. %)	Activation energy, E_a (eV)	Linear regression value, R^2	Conductivity, σ_{rt} (S cm^{-1})
MG10L	90 : 10	0.36	0.98	1.87×10^{-9}
MG20L	80 : 20	0.32	0.96	1.08×10^{-8}
MG30L	70 : 30	0.24	0.98	1.69×10^{-6}
MG40L	60 : 40	0.25	0.96	6.37×10^{-8}

Table 6.1 displays the correlation between the ionic conductivity and activation energy, E_a from which it can be deduced that MG30 samples with higher conductivity always exhibits lower activation energy values. The highest conducting sample MG30L in the salted system possessed the lowest activation energy of 0.24 eV. It can be inferred that E_a (MG30L) < E_a (MG40L) < E_a (MG20L) < E_a (MG10L).

6.2.1 Dielectric studies for MG30–$LiCF_3SO_3$ films

Dielectric constant implies the capacitive nature of the films. Rajendran *et al.* (2010) mentioned that the increase in conductivity with salt content is attributed to the increase in number of free mobile ions and the decrease in conductivity may be due to ion association, which leads to generate more non–conductive neutral ion–pairs. The decrease in conductivity is also in accordance with the decrease in the dielectric loss as shown in Figure 6.6.

Figures 6.6 (a) and (b) show the variation of dielectric constant (ε_r) as a function of frequency for MG30–$LiCF_3SO_3$ polymer electrolytes at 298 K. ε_r is calculated using the equation

$$\varepsilon_r = \frac{Z_i}{\omega C_0 (Z_r^{\,2} + Z_i^{\,2})} \tag{6.3}$$

where Z_r is the real part of impedance; Z_i is the imaginary part of impedance; $C_o = \varepsilon_o A/t$, ε_o is permittivity of free space, A is the effective area of contact between sample and electrolyte, t is the thickness of the sample and $\omega = 2\pi f$ with f as frequency. Dielectric loss (ε_i) is calculated using the equation

$$\varepsilon_i = \frac{Z_r}{\omega C_o (Z_r^{\,2} + Z_i^{\,2})} \tag{6.4}$$

where Z_r, Z_i, ω and C_o are as mentioned above.

From Figure 6.6, the change in dielectric constant with concentration can be readily observed. Such changes have also been observed by Selvasekarapadian *et al.* (2005). It can be observed that the dielectric constant is high at low frequencies due to accumulation of the charge carriers or polarization effect near the electrodes.

At higher frequencies, due to high periodic reversal of the electric field at the interface, the contribution of charge carriers towards the dielectric constant decreases. The decrease in dielectric permittivity with increasing frequency can be associated with the inability of dipoles to rotate rapidly, leading to a lag between the frequency of oscillating dipole and that of the applied field. The increase in dielectric constant is more prominent towards low frequencies due to the effect of electrode polarization. It is observed that the sample that contains 30 wt. % $LiCF_3SO_3$ has the highest dielectric constant and dielectric loss. Therefore, this sample also has the highest conductivity.

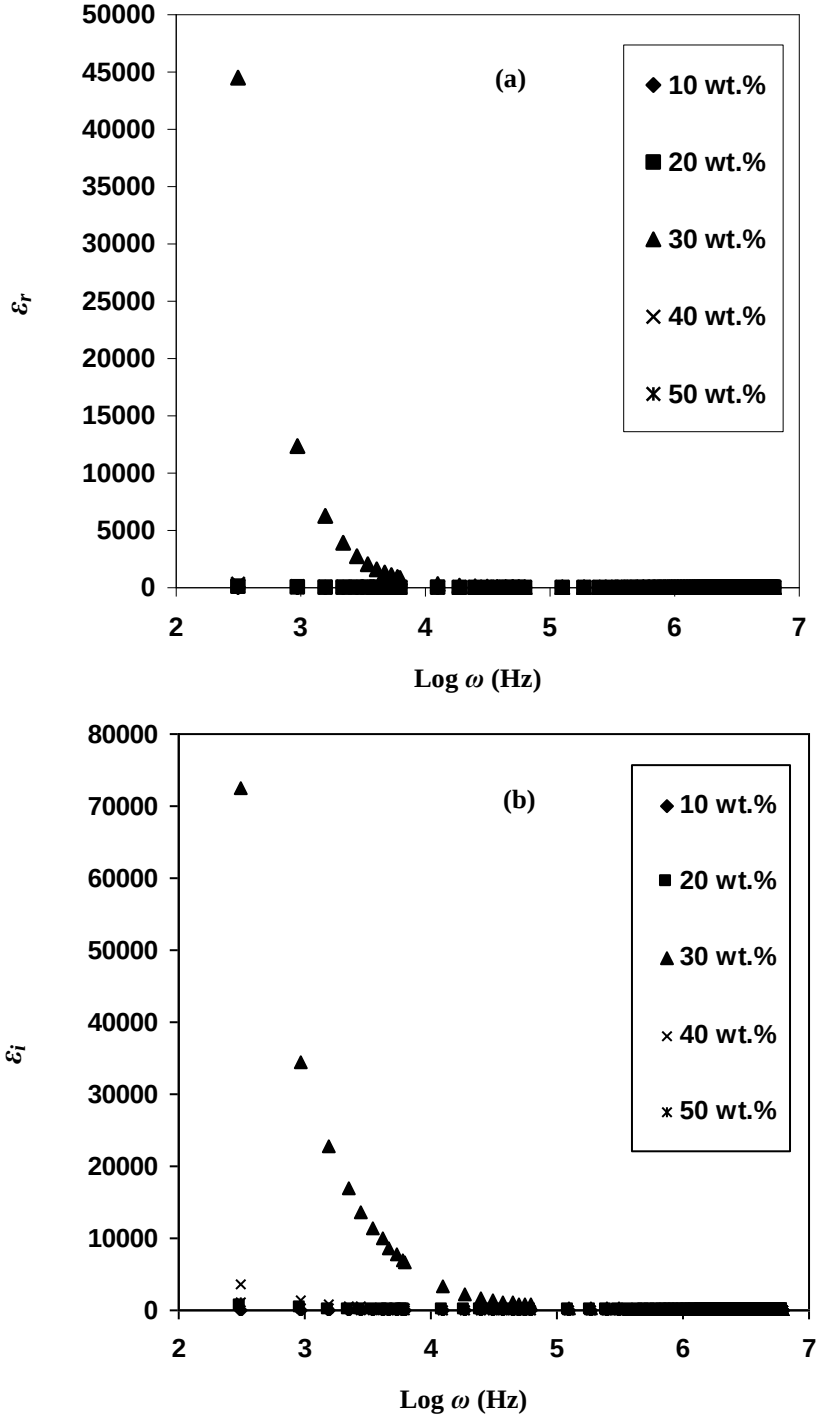

Figure 6.6 Variation of (a) ε_r and (b) ε_i with frequency of MG30–$LiCF_3SO_3$ samples at 298 K

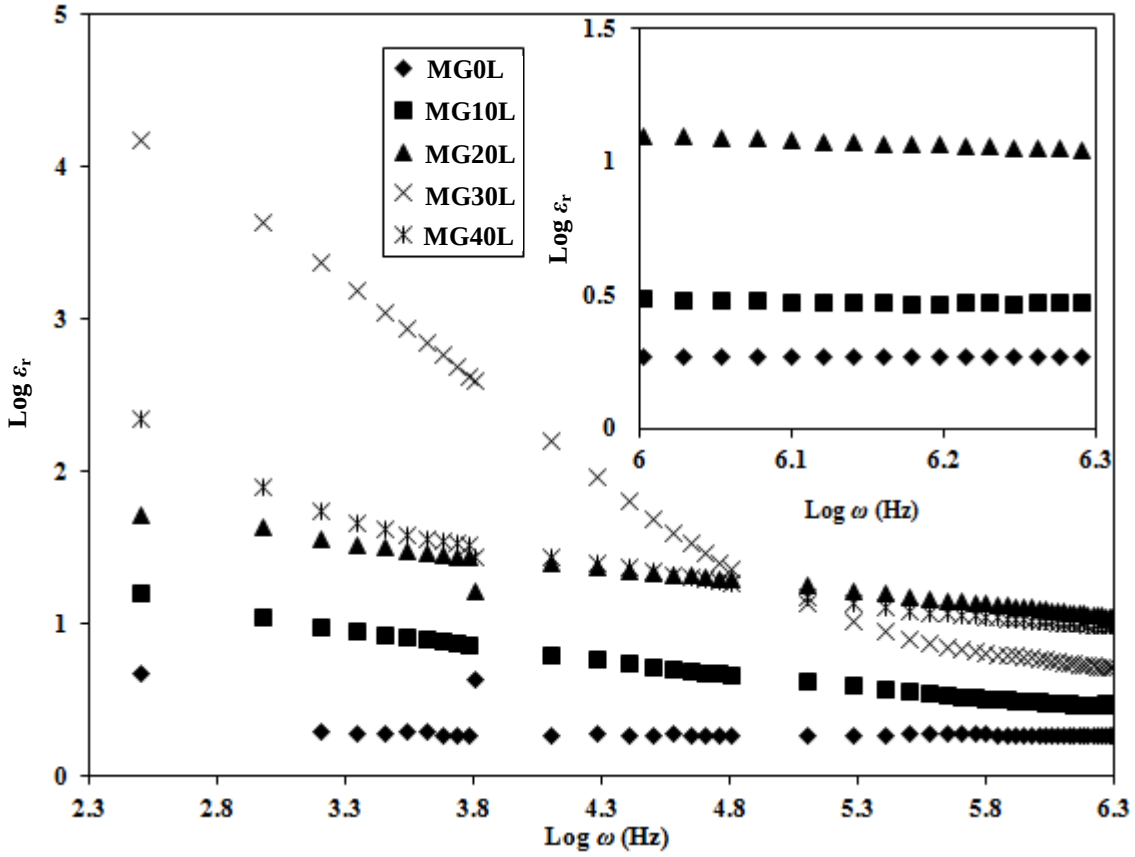

Figure 6.7 Variation of ε_r with frequency for MG30–$LiCF_3SO_3$ samples at 298 K. (Inset shows the enlarged plot at high frequencies)

From Figure 6.7, the variation of ε_r for the salt added samples can be divided into two regions, i.e. low frequency region from 10^2 to 10^6 Hz and the high frequency region above 10^6 Hz. The low frequency region indicates the presence of electrode polarization and the high frequency region which is almost constant represents the bulk region (see inset). Since the dielectric constant for pure MG30 is independent of frequency above 10^6 Hz, the dielectric constant of pure MG30 may therefore be estimated from the high frequency region. Thus, for pure MG30, the dielectric constant, ε_r can be estimated to be 1.86. The polarization effect seems to increase with salt concentration in the high frequency region and therefore the dielectric constant of films containing more than 10 wt. % salt can not be determined.

Figure 6.8 (a) and (b) show the variations of the real ε_r and the imaginary ε_i of the dielectric relaxation curves as a function of log f (Hz) for MG30L polymer electrolyte sample at different temperatures. Both real and imaginary parts of the dielectric increase as frequency decreases. It is found that temperature affects the dielectric property of salted MG30 materials.

Figure 6.9 (a) and (b) show the variations of ε_r and ε_i with temperature at various frequencies for MG30L sample. Both dielectric constant and dielectric loss show temperature dependence and decrease in value with increasing frequency. This observation suggests that the polymer electrolytes are polarized.

The rise in temperature also increases the degree of dipole orientation and consequently enhances the value of dielectric constant. It is clear from the figure that the value of dielectric constant decreases with frequency.

The dielectric loss tangent, tan δ is given by the equation of $\tan\delta = \varepsilon_r / \varepsilon_i$. The relaxation parameters of the complexes can be obtained from the study of tan δ as a function of frequency. Figure 6.10 shows the variation of tan δ as a function of log ω for different amounts of salt in MG30 polymer electrolytes. It has been observed that tan δ increases with increasing frequency and reaches a maximum. Then it decreases for further increase of frequency. For a maximum dielectric loss at a particular temperature, the absorption peak is described by the relation $\omega\tau = 1$ where τ is the relaxation time and ω is angular frequency of the applied signal. The appearance of different sets of relaxation peaks indicates that MG30 shows many different types of relaxation process having different relaxation times (Singh *et al.*, 1998). The relaxation time for MG30L polymer electrolyte is 3.99 x 10^{-6} s at room temperature.

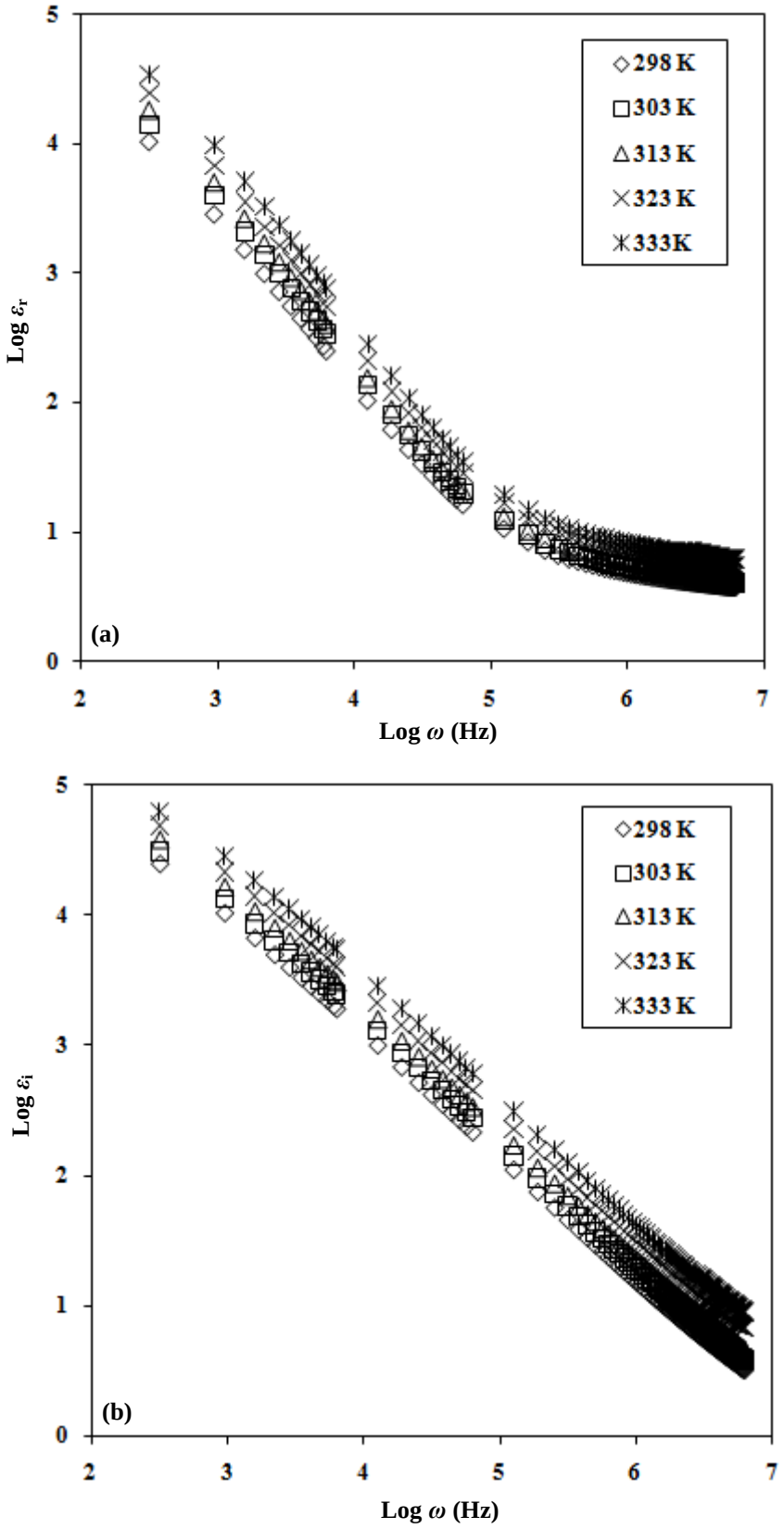

Figure 6.8 Variation of (a) log ε_r and (b) log ε_i with log ω for MG30L sample at different temperatures

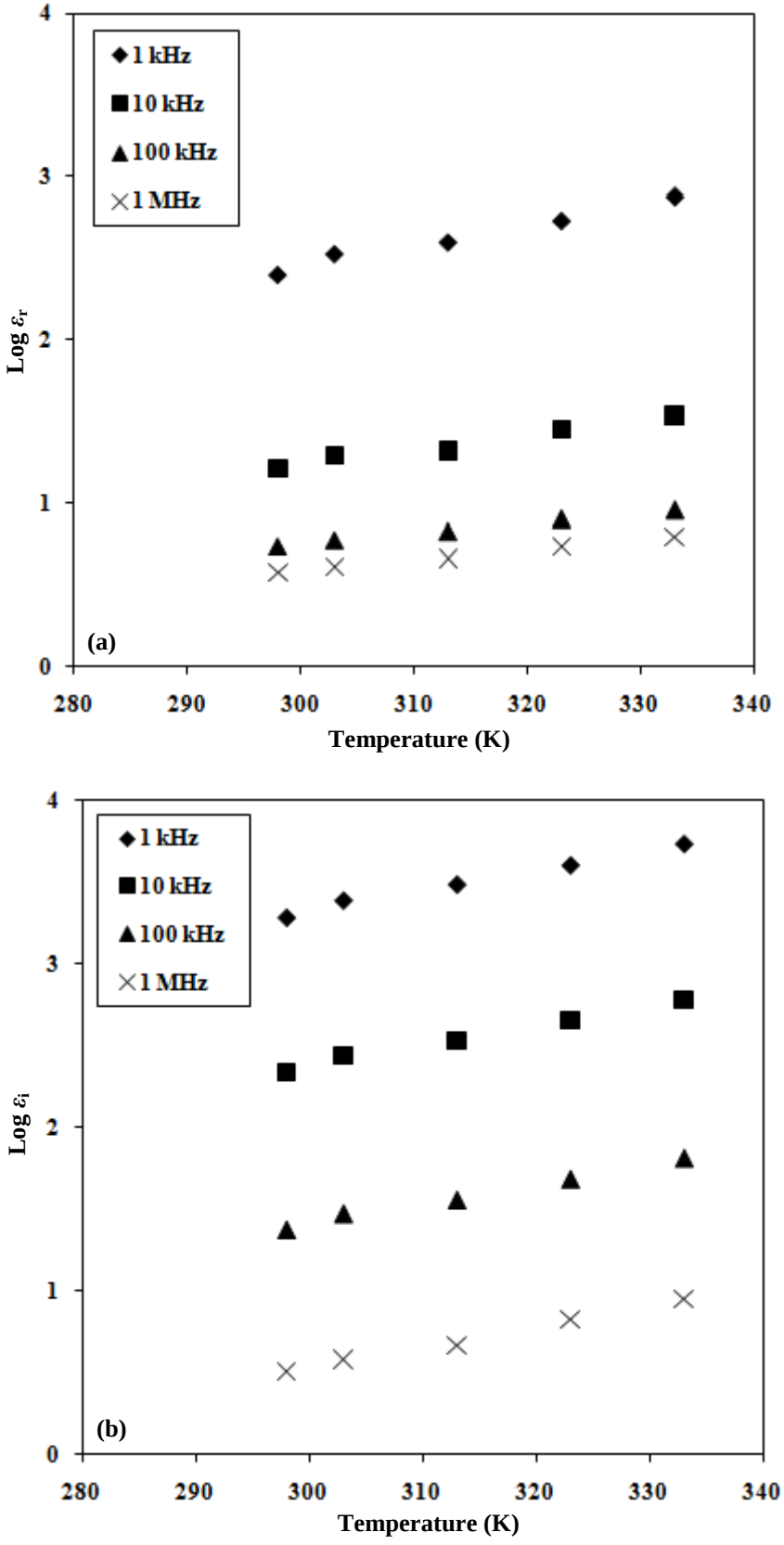

Figure 6.9 Variation of (a) log ε_r and (b) log ε_i with log ω with various frequencies for MG30L sample at different temperatures

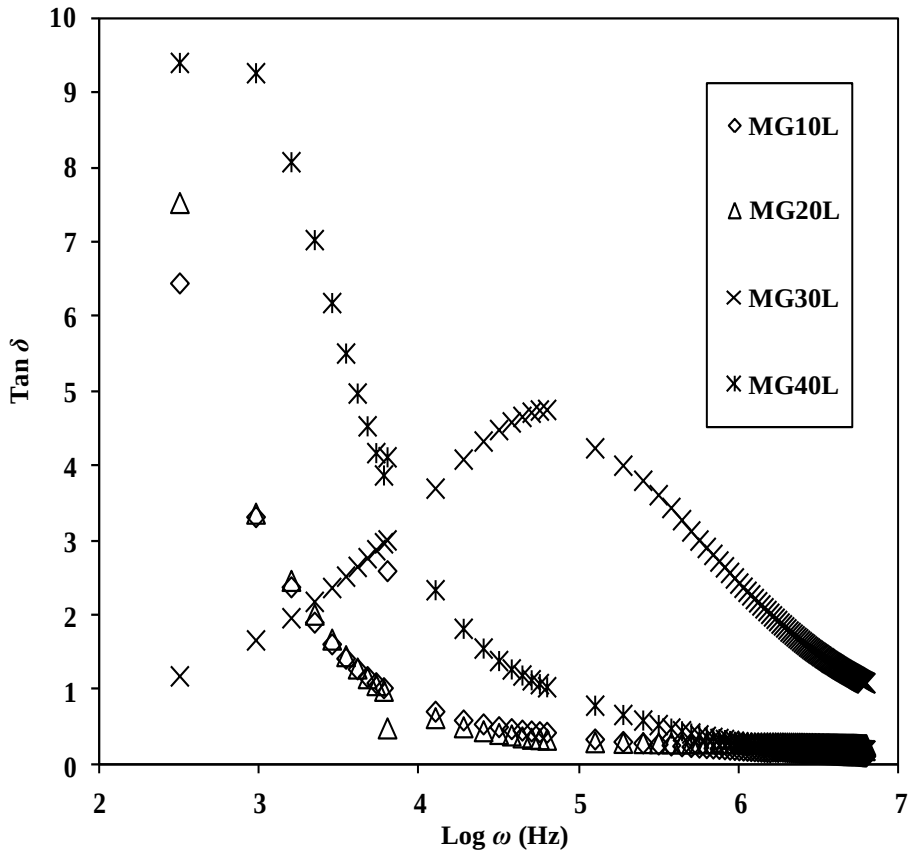

Figure 6.10 Variation of tan δ with frequency for MG30–$LiCF_3SO_3$ polymer electrolytes at 298 K

The occurrence of relaxation time is due to the change in direction of the applied field. The shift of the peaks towards higher frequency suggests shorter relaxation time. It is observed that the peak frequency is shifting towards the higher frequency side with the increase in salt concentration.

Figure 6.11 shows that the variation of tan δ as a function of frequency for MG30L polymer sample at various temperatures. As the temperature increases, the charge carrier has been thermally activated and the loss tangent peak shifts towards higher frequency. This indicates that the relaxation time decreases with increase in temperature. It is seen that the relaxation time, τ decreases with increase in temperature which results in an increase in the ionic conductivity (Vijaya *et al.*, 2012).

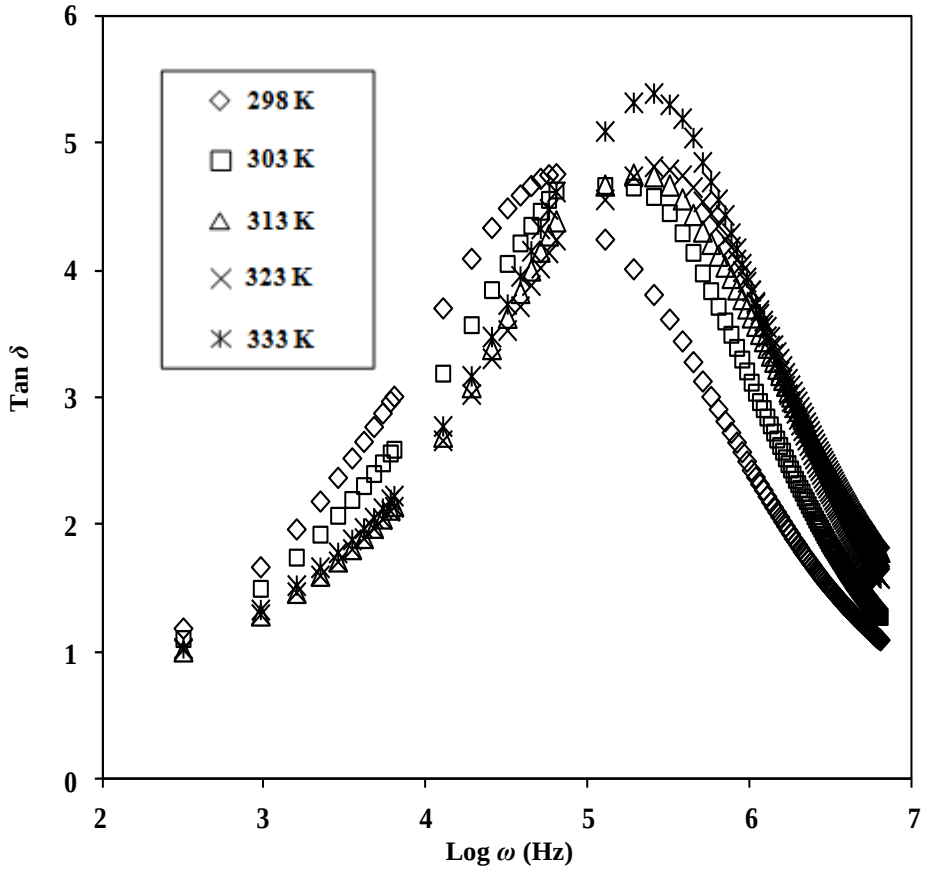

Figure 6.11 Variation of tan δ with frequency for MG30L sample at different temperatures

Figure 6.12 (a) and (b) show the real (M_r) and imaginary (M_i) parts of the electric modulus as a function of log ω where the graphs show a significant decrease in intensity with rising temperature. The equations used were;

$$M_r = \frac{\varepsilon_r}{\varepsilon_r^{\,2} + \varepsilon_i^{\,2}} \tag{6.5}$$

and

$$M_i = \frac{\varepsilon_i}{\varepsilon_r^{\,2} + \varepsilon_i^{\,2}} \tag{6.6}$$

where ε_r *is* the real part of the permittivity and ε_i is the imaginary part of permittivity. M_r and M_i plots for MG30L show an increase at the high frequency end indicating that the polymer electrolyte films are ionic conductors. As the temperature increases, the possible peak maxima shifts to higher frequencies which indicates that the conductivity of the charge carrier has been thermally activated [Ramya *et al.*, 2008]. At low

frequencies, M_r and M_i values approach zero which indicates the capacitive nature of the material. The long tail in the plot may be due to the large capacitance associated with the electrodes [Ramesh *et al.*, 2001; Hema *et al.*, 2009].

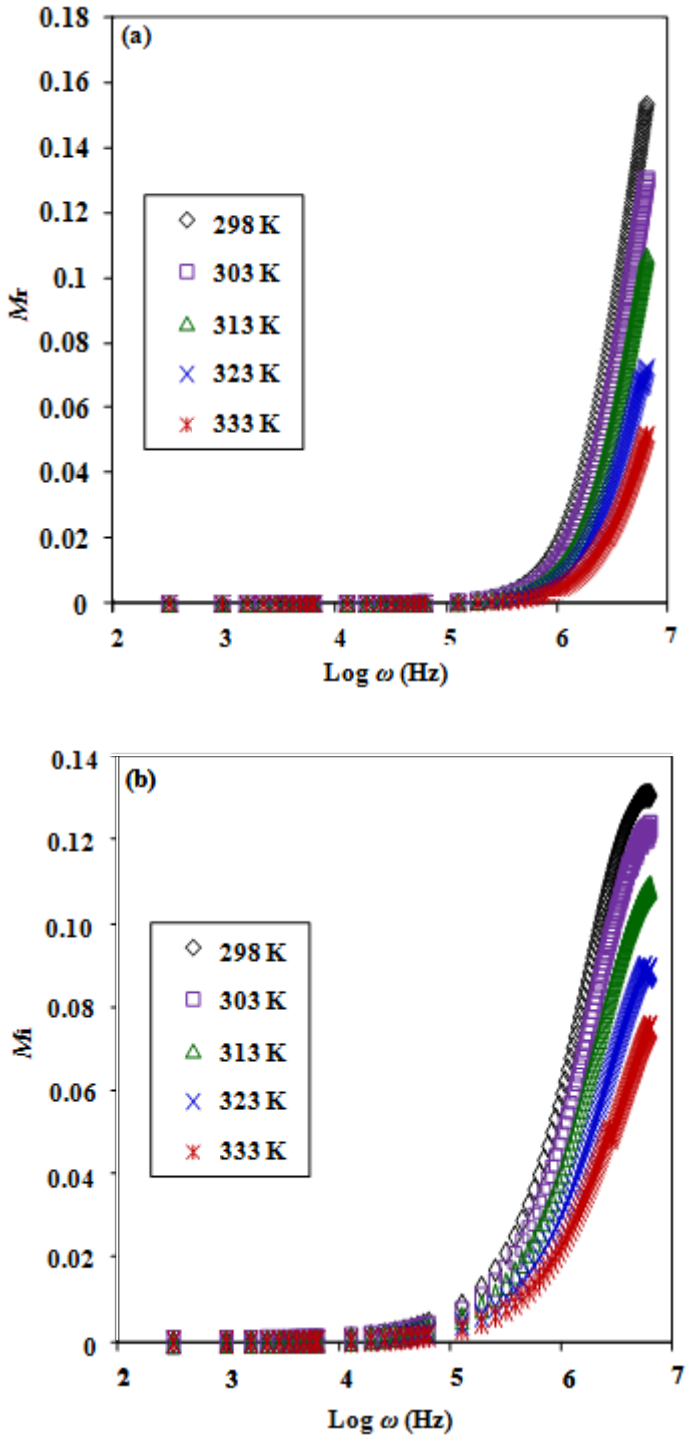

Figure 6.12 Variation of (a) real (M_r) and (b) imaginary (M_i) parts of the electric modulus as a function of log ω for MG30L sample at different temperatures

6.3 Conductivity studies of MG30–$LiCF_3SO_3$–$LiN(CF_3SO_2)_2$ films

Following the results from section 6.2, 70 wt. % MG30–30 wt. % $LiCF_3SO_3$ was prepared in this work and a conductivity of 1.69 x 10^{-6} S cm^{-1} was achieved. Thus double salt polymer electrolytes were prepared with different ratios of $LiCF_3SO_3$ and $LiN(CF_3SO_2)_2$ but the total composition is maintained at 30 wt. %. Figure 6.13 show the Cole–Cole plots of MG30 containing different wt. ratio of $LiCF_3SO_3$: $LiN(CF_3SO_2)_2$. The R_b values were obtained in the same manner as Figure 6.1.

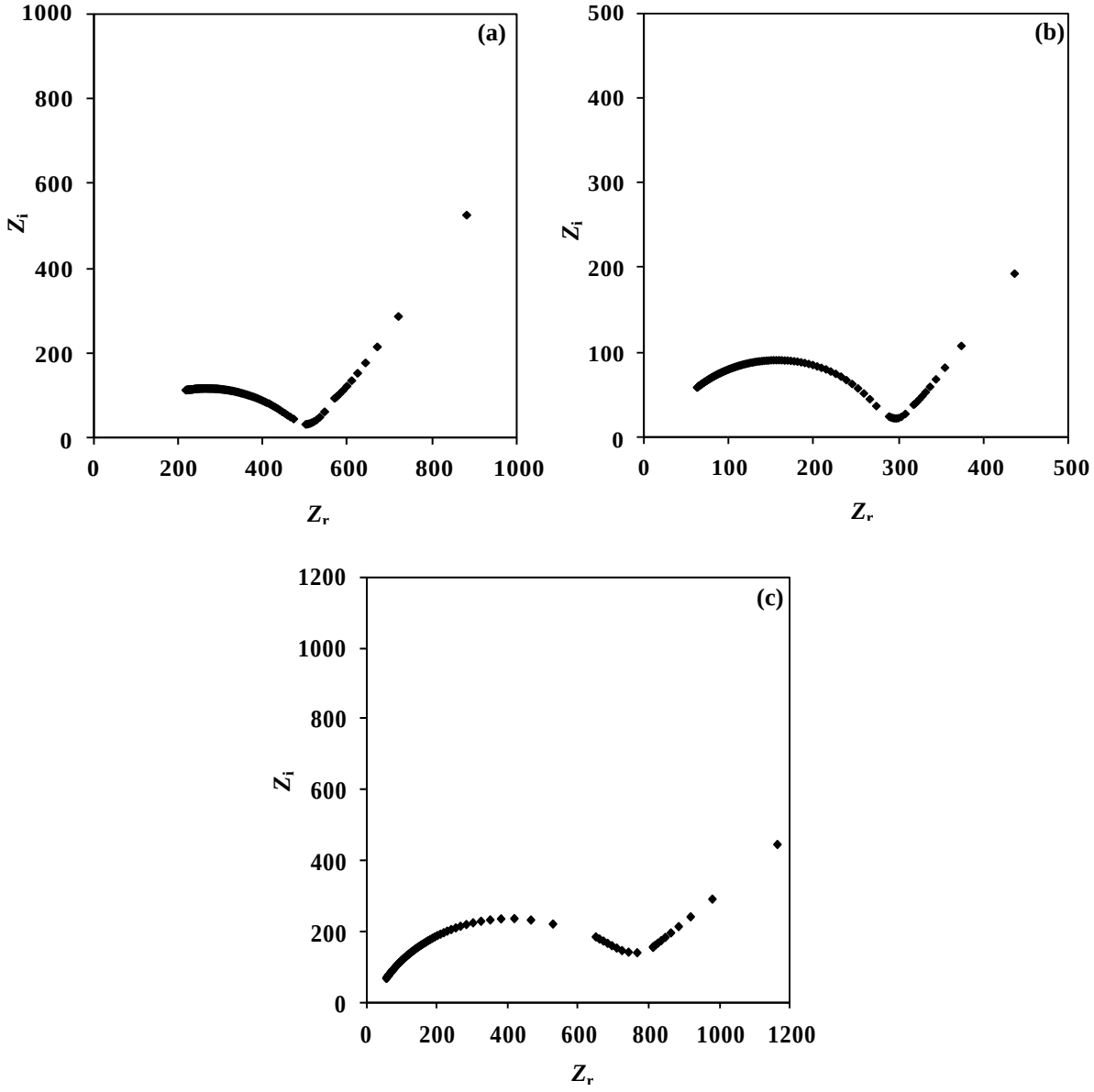

Figure 6.13 Cole–Cole plots of (a) MG10L20I, (b) MG15L15I and (c) MG20L10I at 298 K

The Cole–Cole plots depicted in Figure 6.13 shows the bulk resistance values of the samples decrease following the trend: MG15L15I>MG10L20I>MG20L10I. The temperature dependent conductivity plots of MG30–$LiCF_3SO_3$–$LiN(CF_3SO_2)_2$ samples are shown in Figure 6.14.

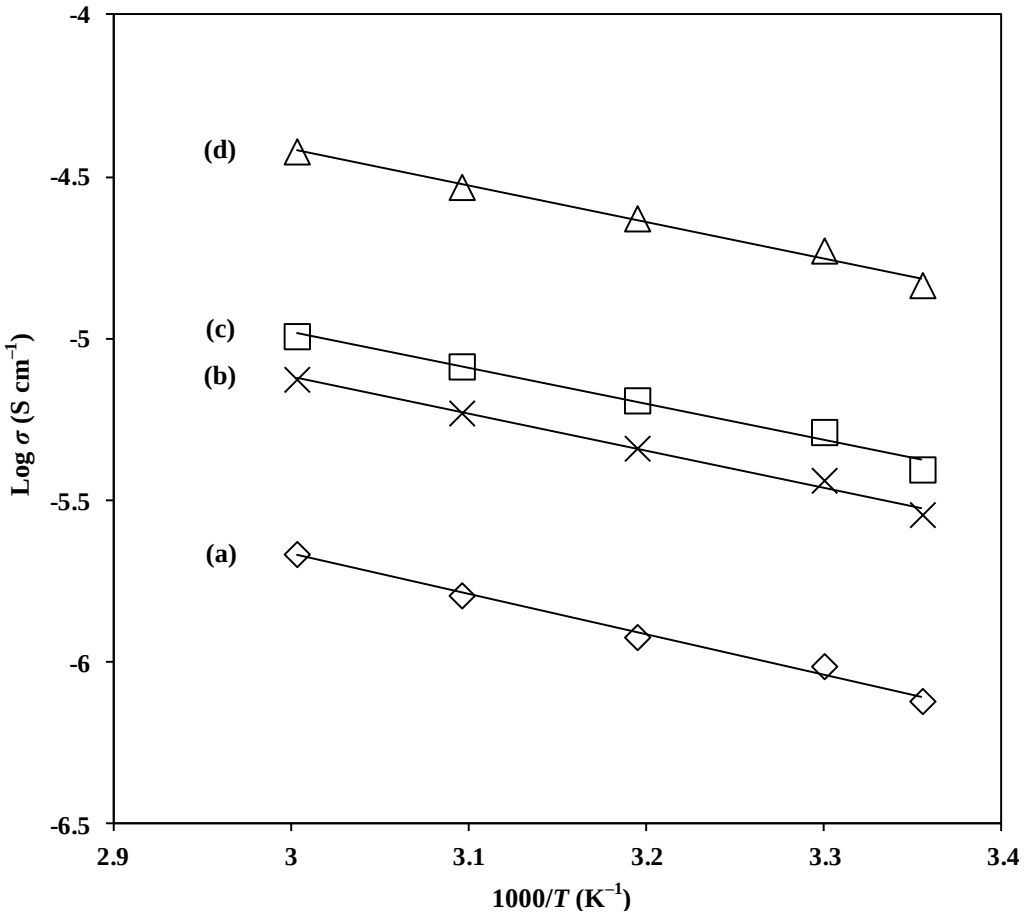

Figure 6.14 Temperature–dependent conductivity plots of (a) MG30L, (b) MG20L10I, (c) MG10L20I and (d) MG15L15I

The linear variation of conductivity versus 1000/*T* plots shown in Figure 6.14 suggests an Arrhenius–type thermally activated process which indicates that there is no phase transition in polymer matrix further more, the regression values are close to unity. The increase in conductivity with temperature is interpreted as hopping mechanism between coordinating sites, local structural relaxations and segmental motions of the polymer salt complexes [Baskaran *et al.*, 2006].

Table 6.2: Conductivity parameters of the MG30–$LiCF_3SO_3$–$LiN(CF_3SO_2)_2$ polymer electrolytes

Designation	Conductivity, σ_{rt} (S cm^{-1})	Linear regression value, R^2	Activation energy, E_a (eV)
MG30L	1.69 x 10^{-6}	0.99	0.24
MG20L10I	2.88 x 10^{-6}	0.98	0.23
MG10L20I	3.93 x 10^{-6}	0.99	0.22
MG15L15I	1.46 x 10^{-5}	0.97	0.21

Table 6.3 reveals that the room temperature ionic conductivity is higher after $LiN(CF_3SO_2)_2$ is introduced in to the systems. The activation energy variation decreased gradually when the conductivity increased. The highest conducting sample MG15L15I in the salted system possessed the lowest activation energy of 0.21 eV. It can be inferred that E_a (MG15L15I) < E_a (MG10L20I) < E_a (MG20L10I) < E_a (MG30L). This is in agreement on our calculation of the lattice energy where the lattice energy is found lower in the bigger size $LiN(CF_3SO_2)_2$ salt.

6.4.1 Dielectric studies of MG30–$LiCF_3SO_3$–$LiN(CF_3SO_2)_2$ films

Figure 6.15 and Figure 6.16 show the variation of (a) ε' and (b) ε'' with log ω for double salted MG30 polymer electrolyte at room temperature and different temperatures. At low frequency, both real and imaginary parts of dielectric rise sharply. As shown in the figures, MG15L15I prevails at higher region and this indicates that it has higher mobile charge carriers for migration compared to other electrolyte samples [Prabu *et al.,* 2010]. This eventually contributes to higher ionic conductivity and it has been proven in Table 6.3.

Figures 6.15 and 6.16 show the dielectric permittivity rise sharply towards low frequencies due to the electrode polarization effects. The low–frequency dispersion region is attributed to the contribution of charge accumulation at the electrode–electrolyte interface [Prabu *et al.*, 2010].

Figure 6.17 show the variation of (a) ε', and (b) ε'' with log ω for various frequencies for MG15L15I sample at different temperatures. It shows the dielectric constant and loss increase with increase of the temperature regardless the frequency range.

The higher values of dielectric constant are expected to be shown in sample with more charge carriers. Both dielectric constant and dielectric loss follow the sequence of MG15L15I > MG10L20I > MG20L10I > MG30L.

This result is consistent with our finding in the conductivity value and the activation energy. Therefore it is reasonable to say that the $LiN(CF_3SO_2)_2$ salt has the ability to dissolve and provide more charge carrier in the polymer electrolyte which may also cause the increase in the relative electric constant and apparently increase in conductivity.

Figures 6.18 and 6.19 depict the graph of loss tangent versus frequency. Trends observed showed that the peaks in loss tangent graph have higher intensity as conductivity of the samples increases and the temperature increases. The relaxation time for MG15L15I polymer electrolyte is 3.16×10^{-5} s at room temperature.

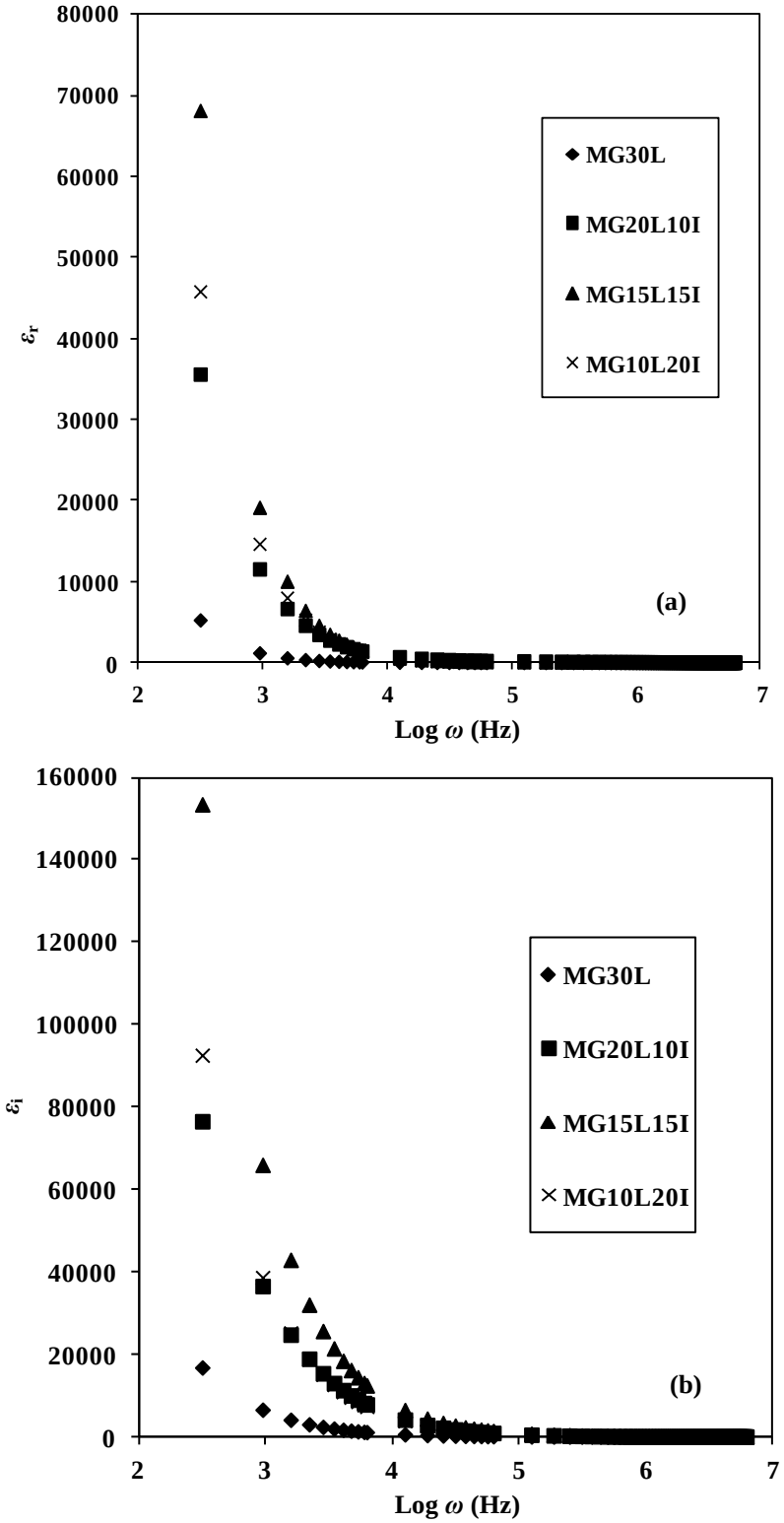

Figure 6.15 Variation of (a) ε_r and (b) ε_i with log ω of MG30L sample and MG30–$LiCF_3SO_3$–$LiN(CF_3SO_2)_2$ polymer electrolyte system at different temperatures

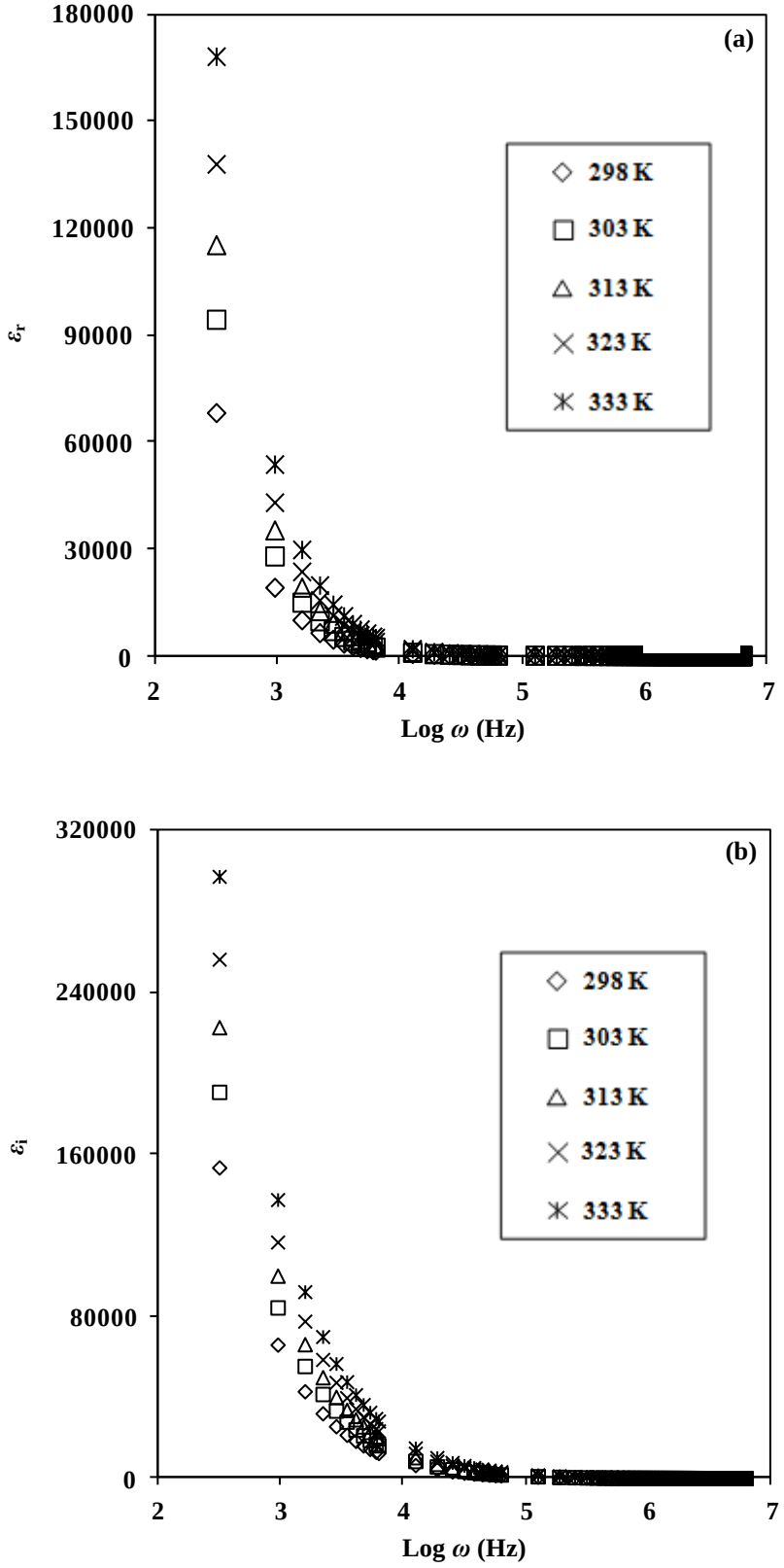

Figure 6.16 Variation of (a) ε_r and (b) ε_i with log ω for MG15L15I sample at different temperatures

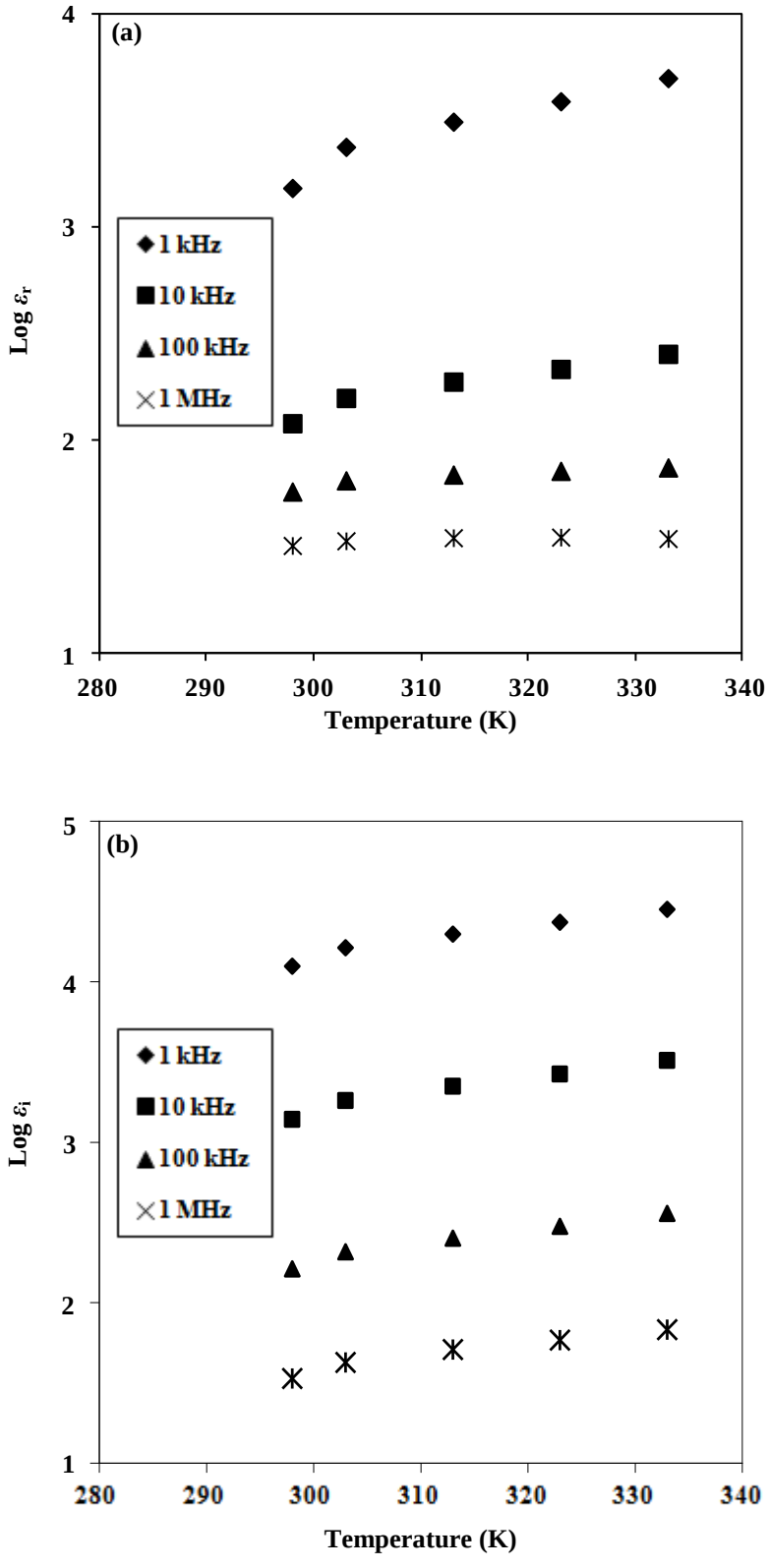

Figure 6.17 Variation of (a) ε_r and (b) ε_i with log ω for various frequencies for MG15L15I sample at different temperatures

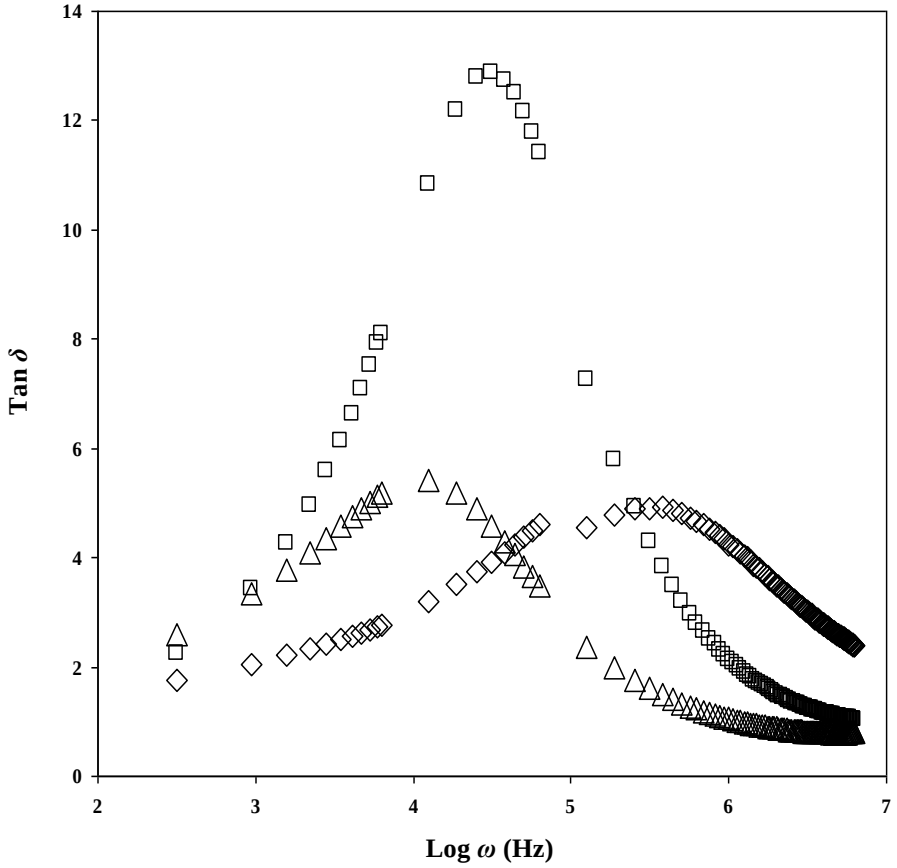

Figure 6.18 Variation of tan δ with frequency for (a) MG20L10I (b) MG15L15I and (c) MG10L20I samples at 298 K

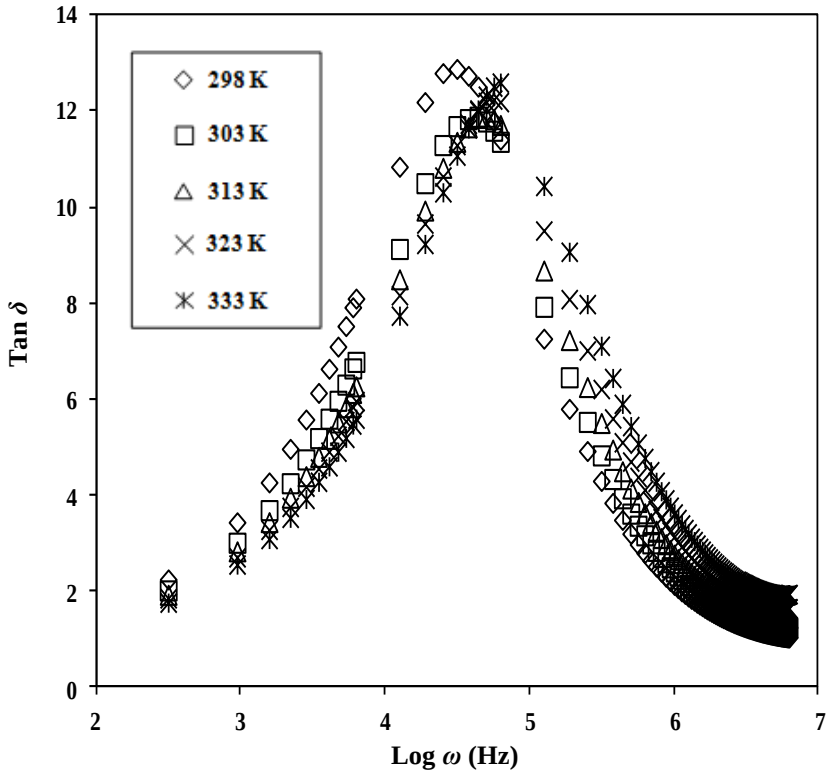

Figure 6.19 Variation of tan δ with frequency for MG15L15I sample at different temperatures

Figure 6.20 (a) and (b) show the frequency dependence of the real (M_r) and imaginary (M_i) parts of modulus formalism.

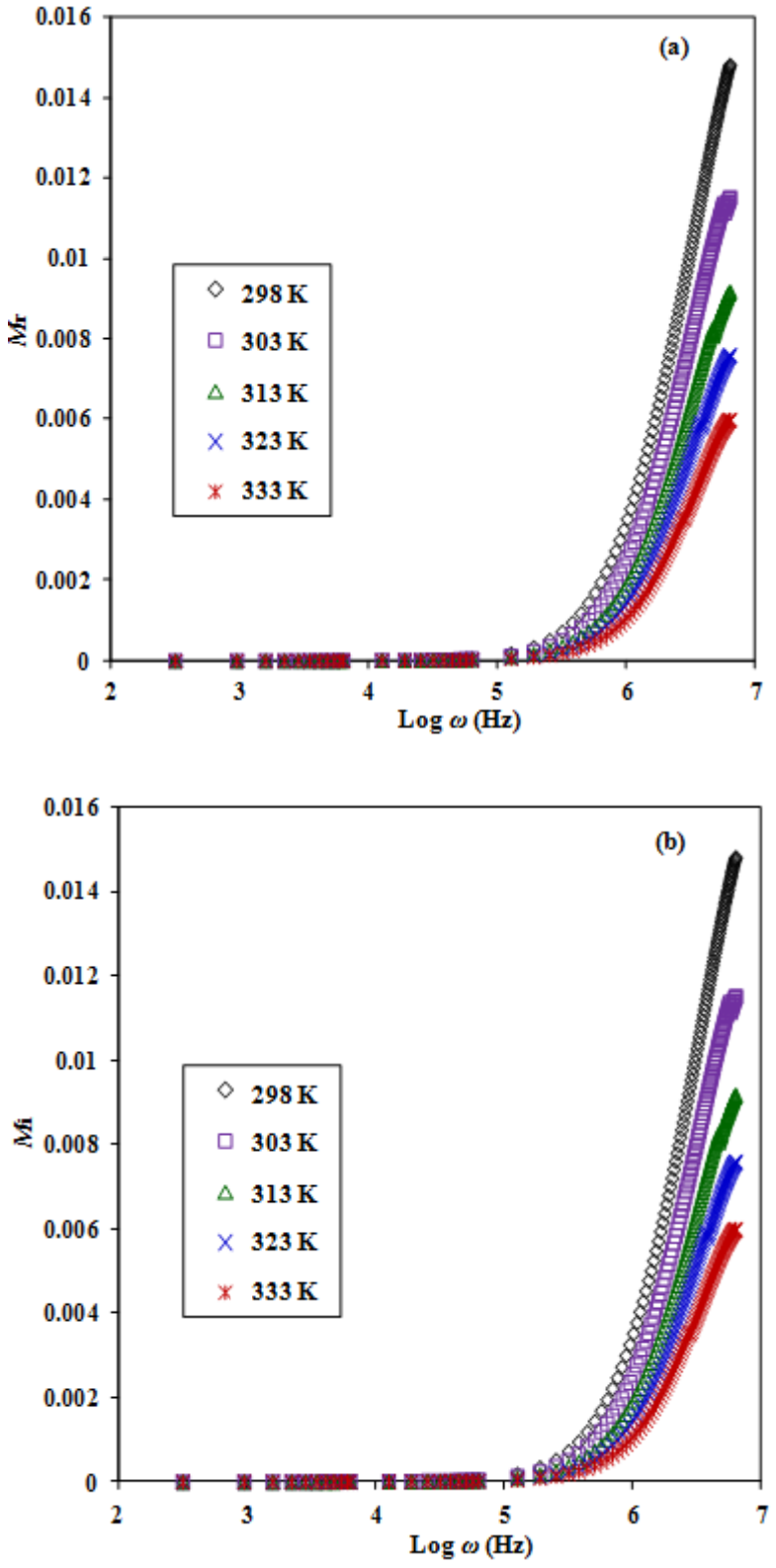

Figure 6.20 Variation of (a) real (M_r), and (b) imaginary (M_i) parts of the electric modulus as a function of log ω for MG15L15I sample at different temperatures

From Figure 6.20, it can be observed that M_r and M_i increase towards high frequencies. The presence of the peaks in the modulus formalism at higher frequencies for all polymer complexes and temperatures imply that the polymer electrolyte films are ionic conductors. The peaking curve at higher frequencies may be caused by bulk effect [Ramesh *et al.,* 2007]. M_r and M_i decrease with a long tail towards low frequencies showing the fact that the electrode polarization phenomena make a negligible contribution. The long tail is probably the results of the large capacitance associated with the electrode.

6.4 Conductivity studies of MG30–$LiCF_3SO_3$–PEG200 films

Figure 6.21 represents the Cole–Cole plot for the 70 wt. % MG30–30 wt. % $LiCF_3SO_3$–PEG200 plasticized polymer electrolyte systems. It is noted that the semicircle in high frequency region gradually disappears as the content of PEG200 increases, and completely disappears in polymer electrolytes containing more than 10 wt. % PEG200 as can be observed in Figures 6.21 (c). The disappearance of the semi–circle at higher conducting films suggests that only the resistive component of the polymer prevails.

Figure 6.22 shows the impedance plot for sample with 10 wt. % concentration of PEG200 at different temperatures. It can be found that the bulk resistance decreases as the temperature increases which in turn leads to the increase in conductivity of the polymer electrolytes. Figure 6.23 depicts the effect of PEG200 content on the ionic conductivity of 70 wt. % MG30–30 wt. % $LiCF_3SO_3$ polymer electrolyte system at room temperature. Figure 6.23 clearly shows that the addition of plasticizer has

remarkable effect on the conductivity of the electrolyte. The highest conductivity is 3.65 x 10^{-4} S cm^{-1} at ambient temperature for MG30L–10P sample.

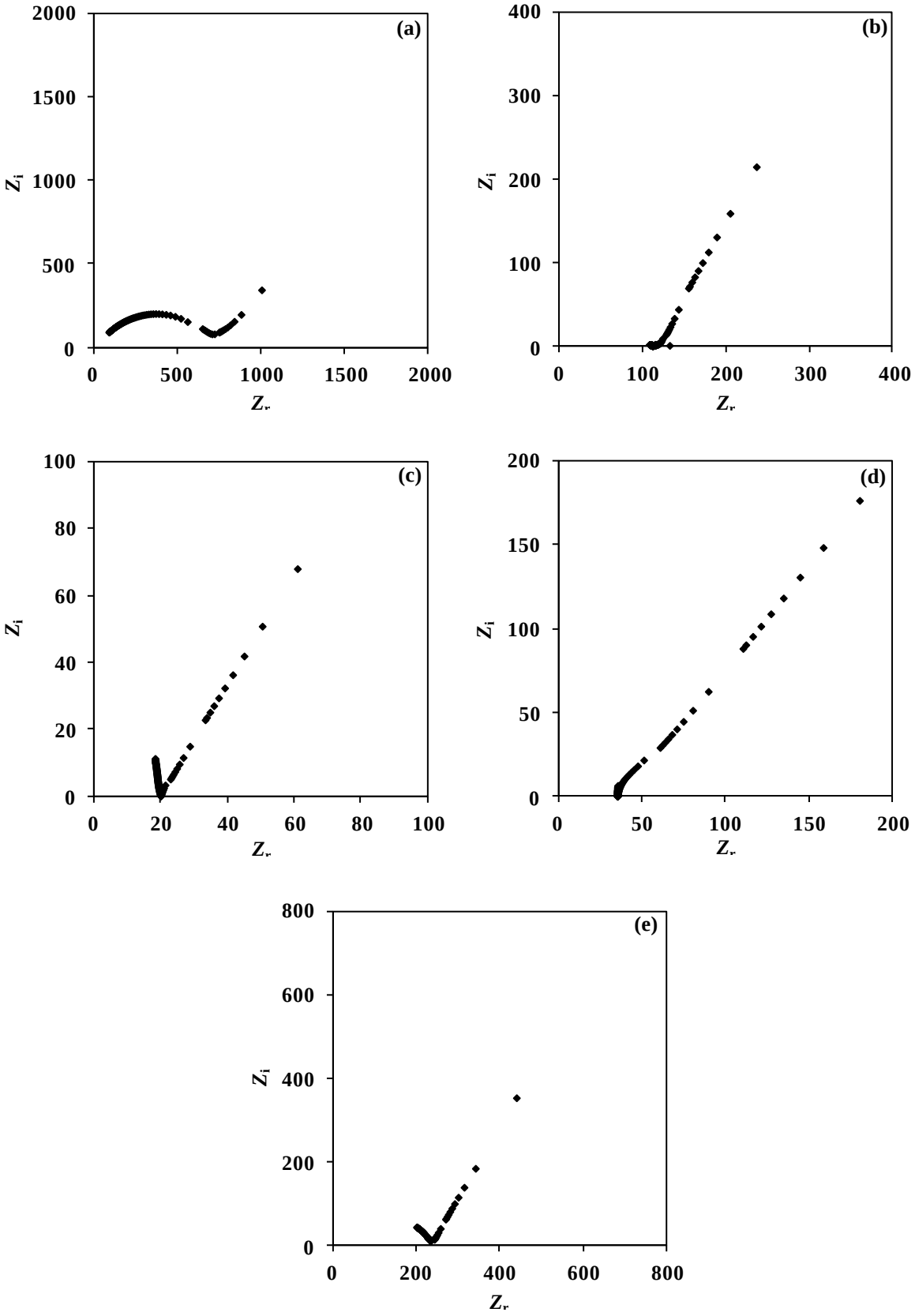

Figure 6.21 Cole–Cole plots of (a) MG30L–5P, (b) MG30L–7P, (c) MG30L–10P, (d) MG30L–20P and (e) MG30L–30P at 298 K

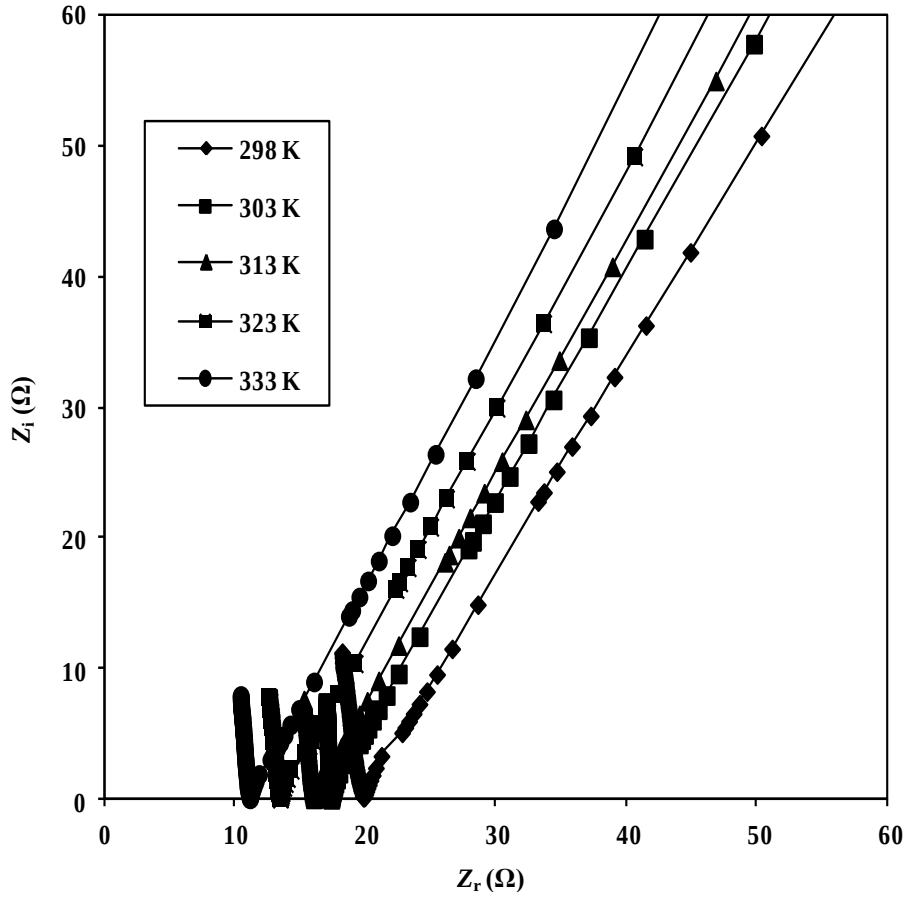

Figure 6.22 Cole–Cole plots of MG30L–10P polymer electrolyte film at different temperatures

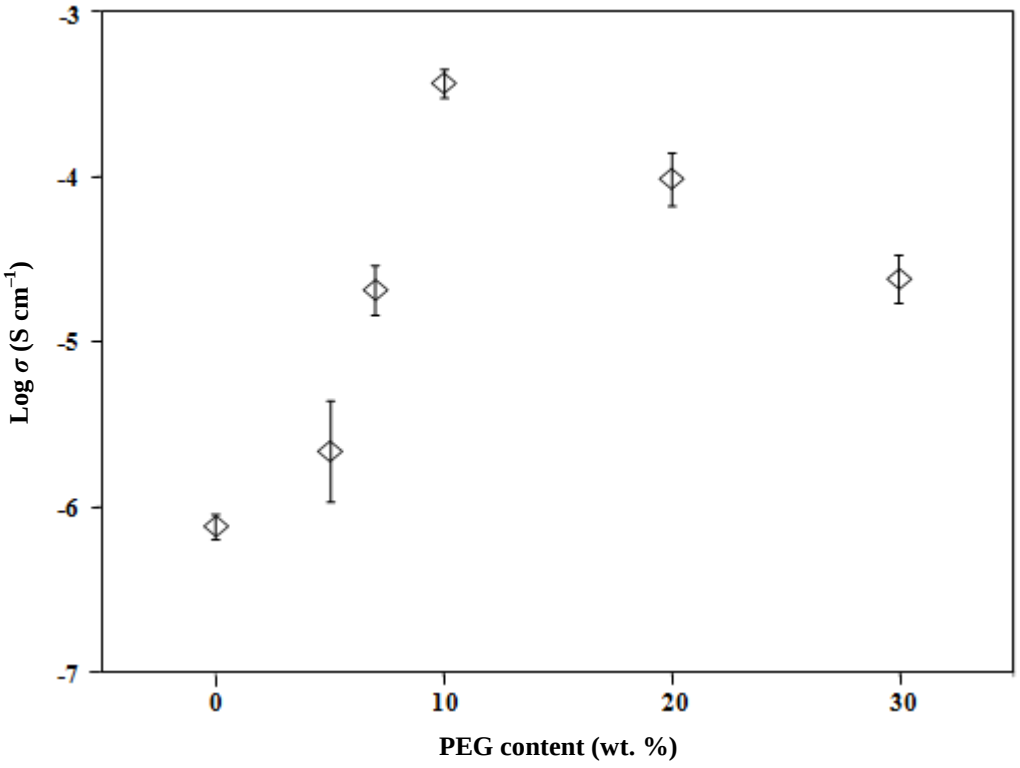

Figure 6.23 Plot of log σ versus PEG content for (1–x) [70 wt. % MG30–30 wt. % $LiCF_3SO_3$]–x wt. % PEG200 polymer electrolyte system at 298 K

Figure 6.24 represents the temperature–dependent conductivity for all compositions of (1–*x*) wt. % [70 wt. % MG30–30 wt. % $LiCF_3SO_3$]–*x* wt. % PEG200 polymer electrolytes. It can be observed that the conductivity of the membranes increases with increasing temperature for all compositions indicating the Arrhenius type thermally activated process.

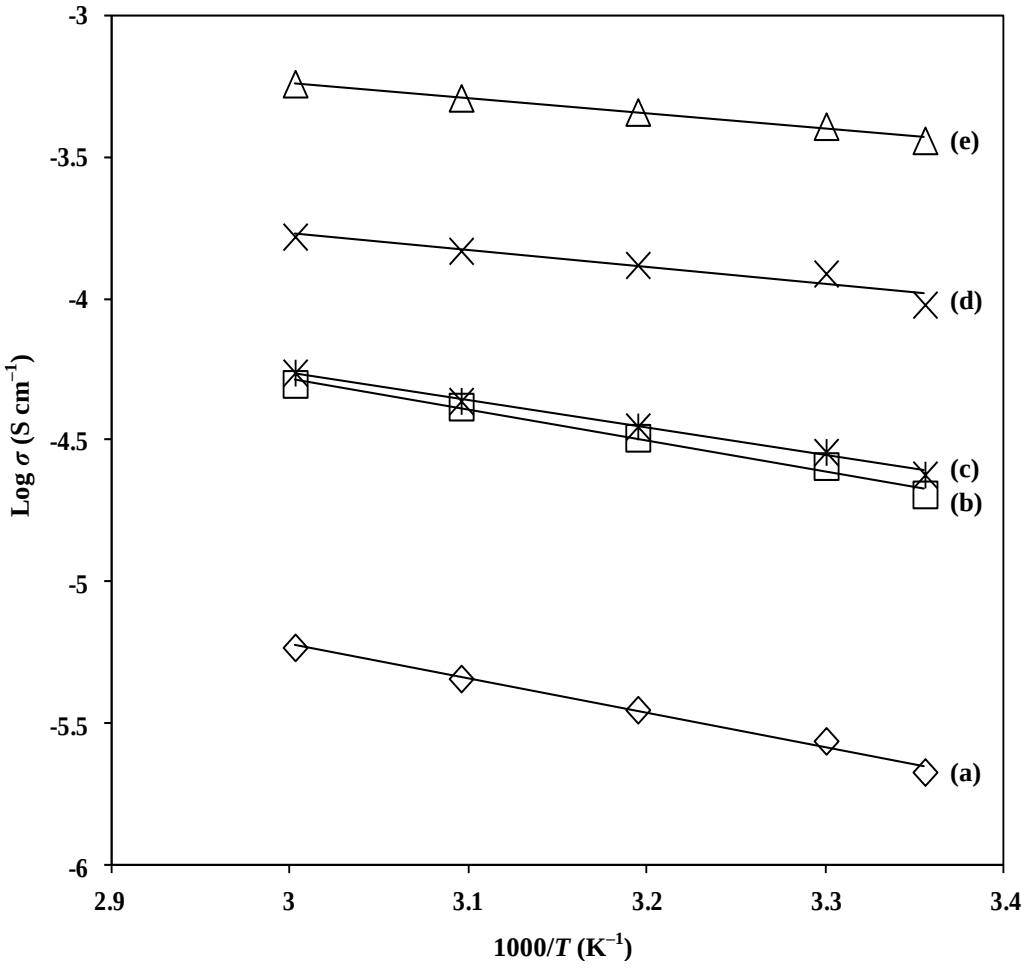

Figure 6.24 Temperature–dependent conductivity plots of (a) MG30L–5P, (b) MG30L–7P, (c) MG30L–30P, (d) MG30L–20P and (e) MG30L–10P samples

Table 6.3 displays the conductivity parameters of the MG30–$LiCF_3SO_3$–PEG200 polymer electrolyte system.

Table 6.3: Conductivity parameters of the MG30–$LiCF_3SO_3$–PEG200 plasticized polymer electrolytes

Designation	Conductivity, σ_{rt} (S cm^{-1})	Linear regression value, R^2	Activation energy, E_a (eV)
MG30L5P	2.15×10^{-6}	0.99	0.24
MG30L7P	2.03×10^{-5}	0.98	0.21
MG30L10P	3.65×10^{-4}	0.99	0.11
MG30L20P	9.62×10^{-5}	0.93	0.12
MG30L30P	2.38×10^{-5}	0.98	0.19

The E_a for MG30L10P has been calculated to be 0.11 eV and the activation energy increase with further increase of salt concentration. It is also observed that lower activation energy is a characteristic of a solid polymer electrolyte film having a higher value of ionic conductivity [Ramesh and Arof, 2011]. It can be inferred that E_a (MG30L10P) < E_a (MG30L20P) < E_a (MG30L7P) < E_a (MG30L30P) < E_a (MG30L5P).

6.4.1 Dielectric studies of MG30–$LiCF_3SO_3$–PEG200 films

The variation of dielectric constant and dielectric loss with MG30–$LiCF_3SO_3$ films containing various amounts of PEG200 is depicted in Figure 6.25.

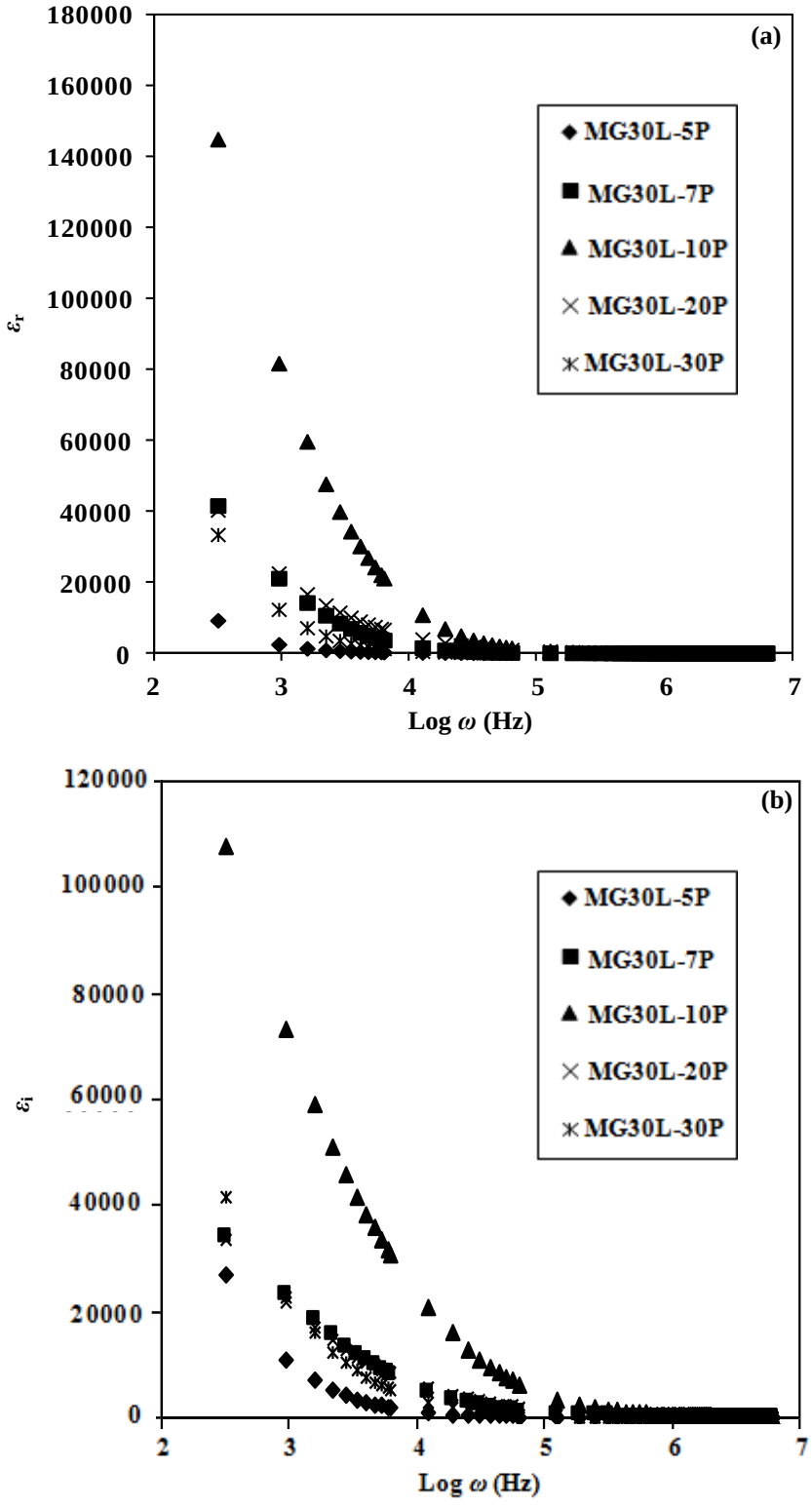

Figure 6.25 Variation of (a) ε_r and (b) ε_i with log ω for (1–*x*) wt. % [70 wt. % MG30–30 wt. % $LiCF_3SO_3$] – *x* wt. % PEG200 (where *x* = 5, 7, 10, 20, 30) polymer electrolyte at different temperatures

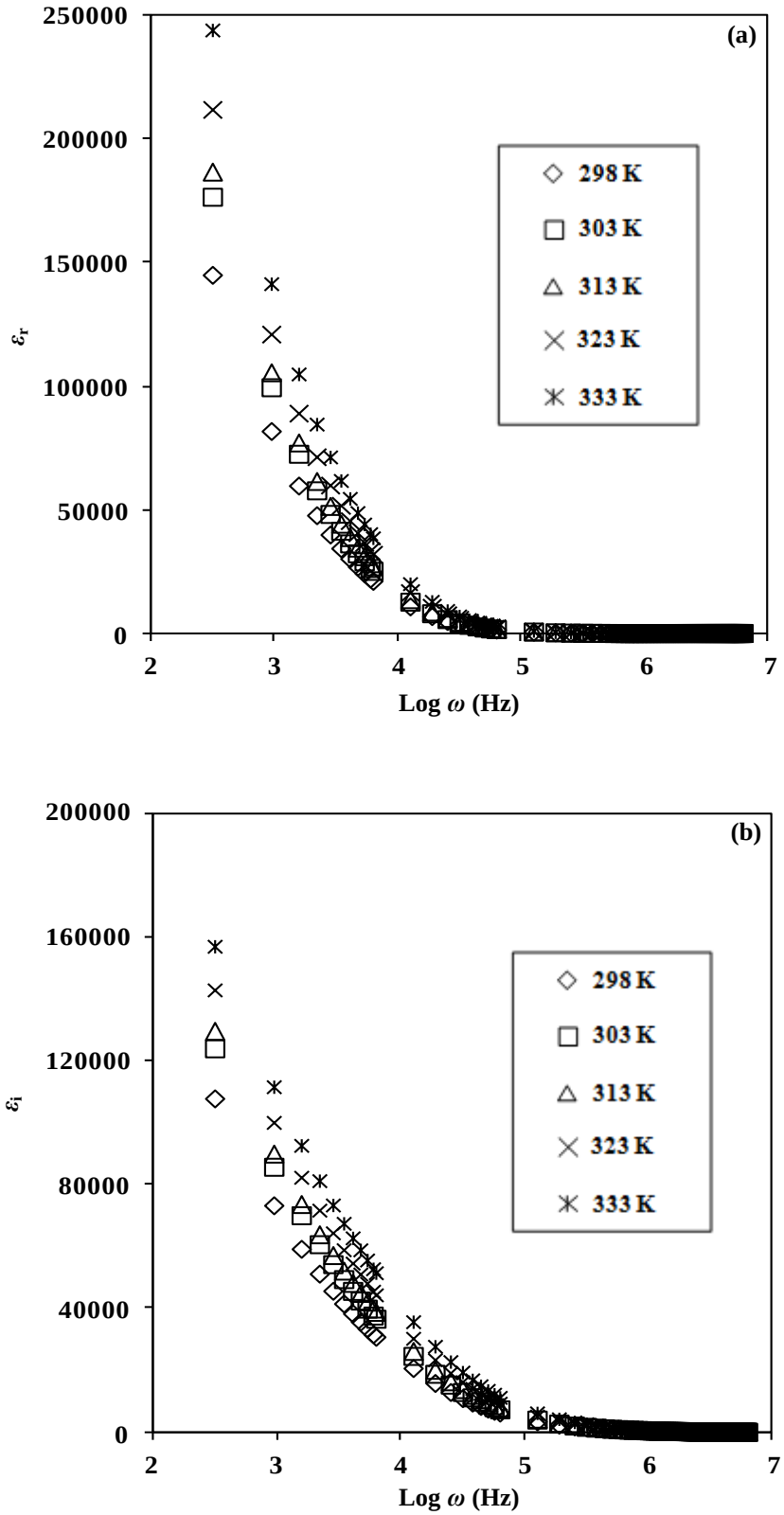

Figure 6.26 Variation of (a) ε_r and (b) ε_i with log ω for MG30L–10P sample at different temperatures

From the characteristic curves in Figures 6.25 and 6.26, the value of the dielectric constant decreases with rising frequency and this value is large at elevated temperatures in comparison to room temperature. The higher value of dielectric constant for PEG200 plasticized MG30 system is due to the enhanced charge carrier density at the space charge accumulation region and the dielectric constant decreases at higher frequencies due to the high periodic reversal of applied field [Nithya *et al.*, 2011]. Addition of PEG200 has modified MG30's physical properties such as flexibility, microstructure, viscosity and internal friction and overall resulting in an increase in chain segmental mobility, thus increase in the dielectric constant and hence conductivity of the polymer [Polu and Kumar, 2011].

Figure 6.27 reveals that the values of dielectric constant increases gradually with temperature. The increase in dielectric constant and dielectric loss above the room temperature may be due to the expansion of the lattice and excitation of charge carriers, which are likely to be present inside the imperfection sites inside the specimen. This molecular alignment of chains may cause the observed increase to the polarization of the system [Chandar *et al.*, 1999].

Figure 6.28 shows the shift of the peak towards high frequency side. This suggests that shorter relaxation time occur with the increase in PEG200 concentration. It is also observed that the intensity of the peak of tan δ also increases with increase of temperature, Figure 6.29. The relaxation time for MG30L–10P polymer electrolyte is 1.58×10^{-6} s at room temperature.

Complex electric modulus has been used to investigate the conductivity relaxation phenomena because it has the ability to suppress the effects of electrode

polarization to give a clearer picture of electrical property. No relaxation peak is observed in Figure 6.30 (a) and (b).

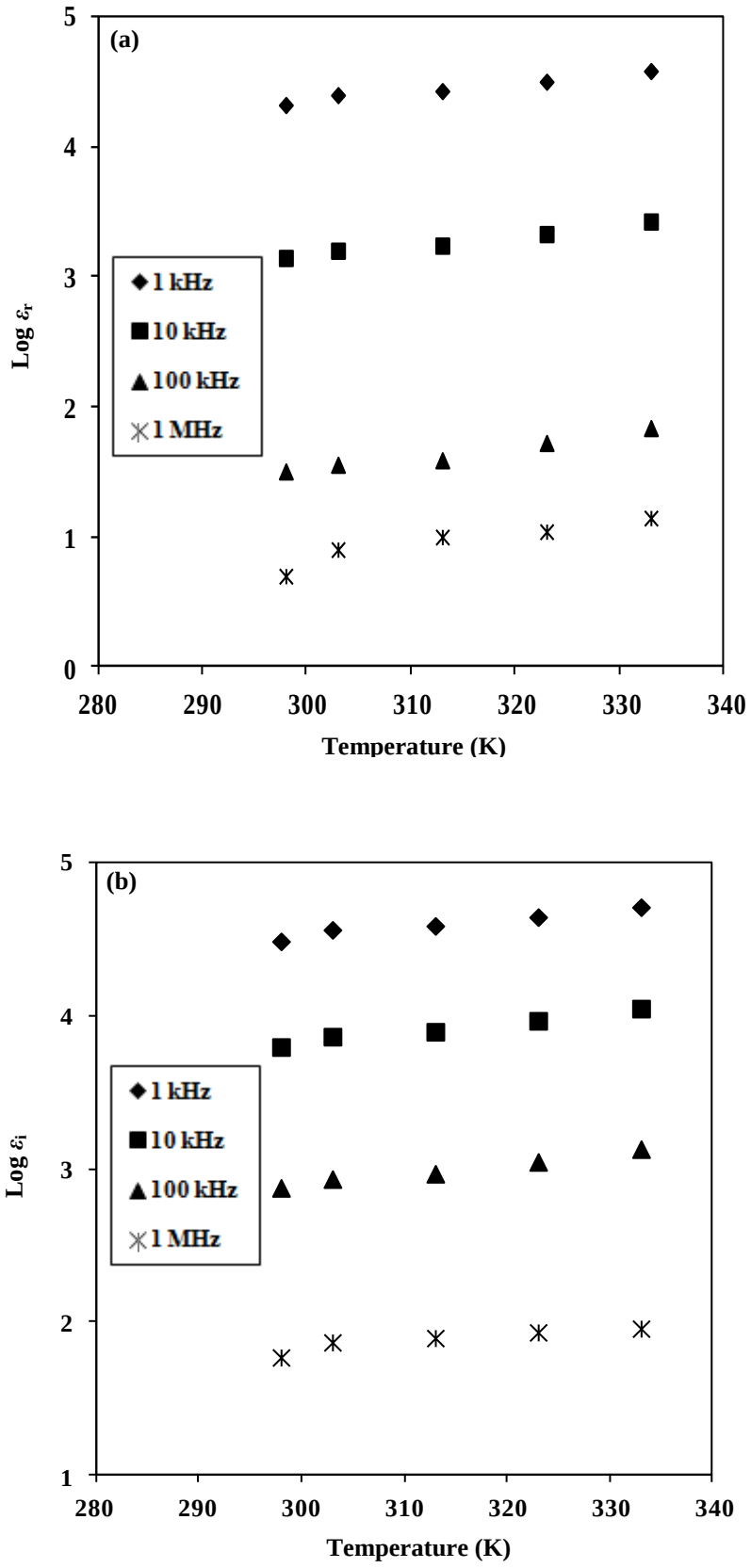

Figure 6.27 Variation of (a) ε_r and (b) ε_i with log ω for various frequencies for MG30L–10P sample at different temperatures

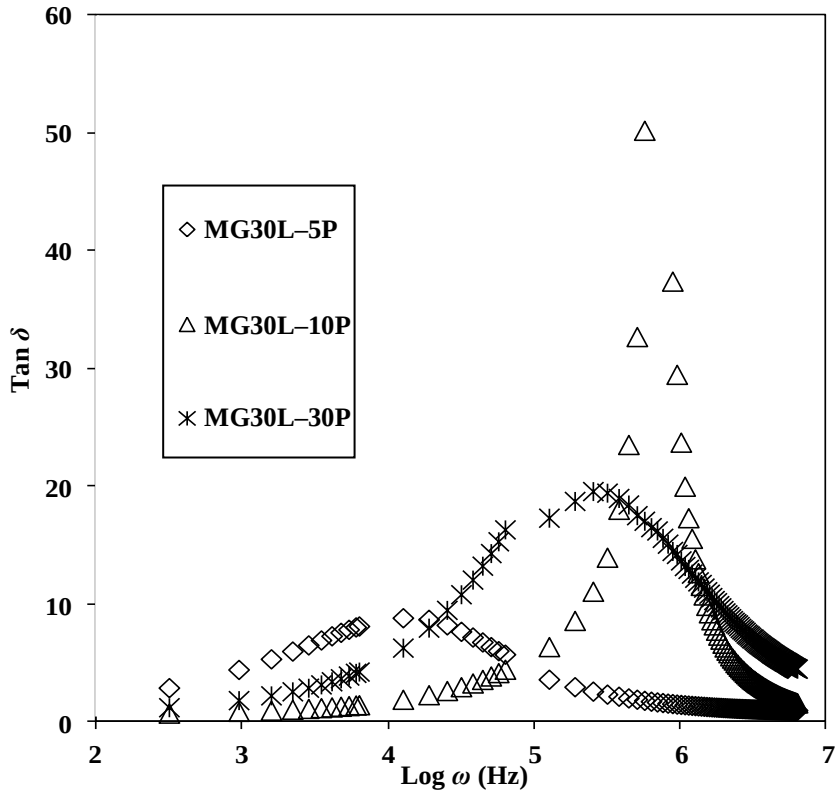

Figure 6.28 Variation of tan δ with frequency for various amounts of PEG200 in 70 wt. % MG30–30 wt. % $LiCF_3SO_3$ polymer electrolytes at 298 K

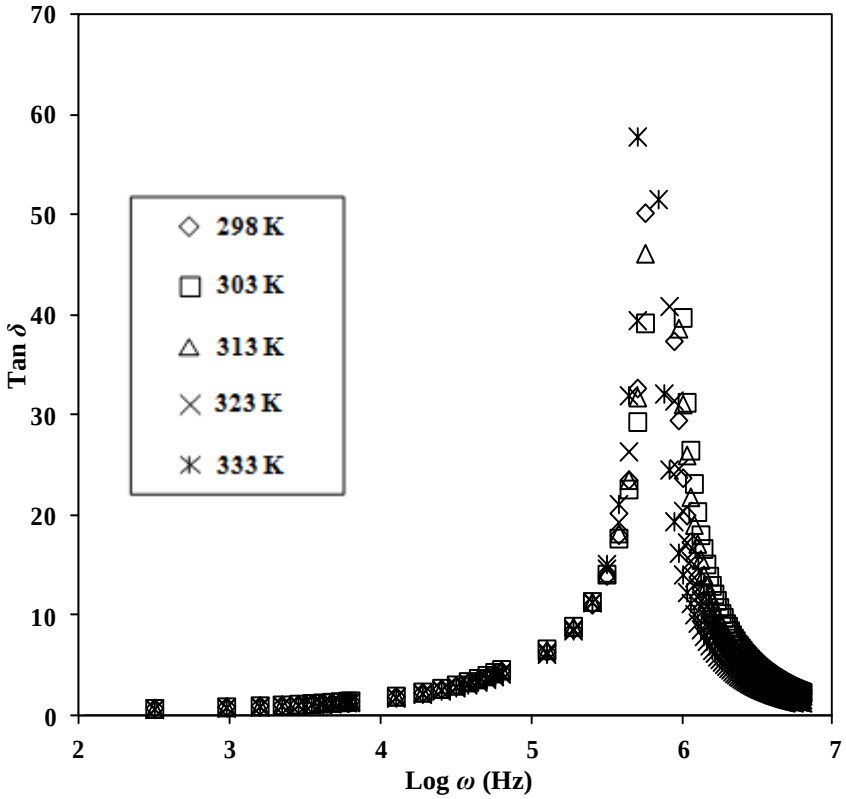

Figure 6.29 Variation of tan δ with frequency for MG30L–10P sample at different temperatures

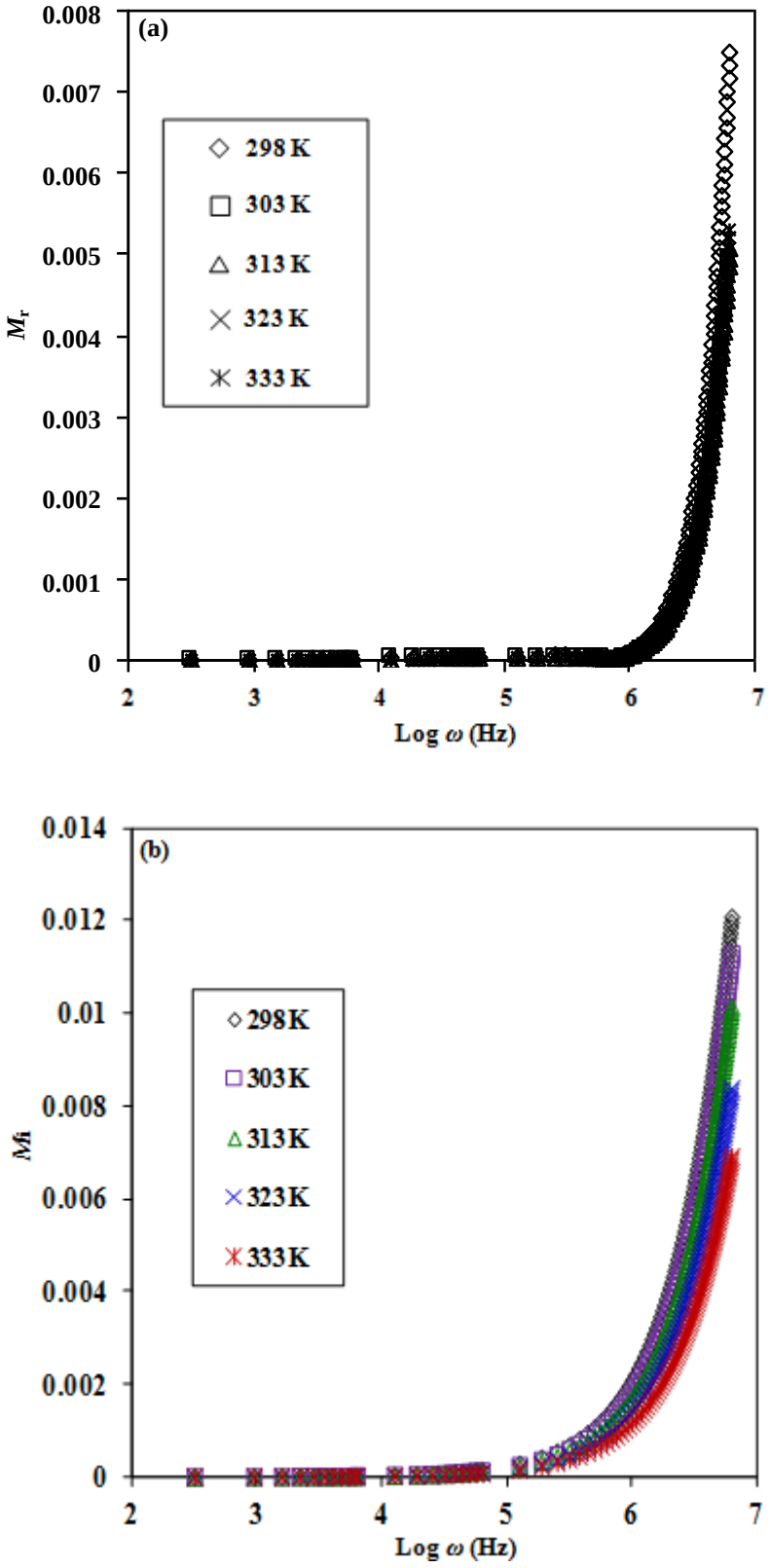

Figure 6.30 Variation of (a) real (M_r), and (b) imaginary (M_i) parts of the electric modulus as a function of log ω for MG30L–10P sample at different temperatures

A long tail observed at low frequency region may be attributed to the large capacitance associated with the electrodes. An increase in dielectric modulus at high frequency end has been observed which may be attributed to bulk effect. At low frequencies, the value decrease to zero indicating a negligible electrode polarization.

An apparent observation is observed in Figure 6.30 (a). For *M*', all the curves demonstrate superposition features in temperature regime at high frequency and thus disclose that the modulus spectral posses temperature independent ability and excellent electrochemical stability of MG30L10P [Austin Suthanthiraraj *et al.*, 2009].

6.4.2 Transference number measurements

The transference numbers corresponding to ionic (t_{ion}) and electronic (t_{ele}) transport has been evaluated in the highest conducting MG30–$LiCF_3SO_3$–PEG electrolyte sample by means of Wagner polarization technique. In this technique, the dc current is monitored as a function of time on application of a fixed dc voltage across the sample with blocking electrodes. Stainless steel (SS) and lithium metal foil (Li) were employed as the blocking and non–blocking electrodes, respectively. Cells having the configurations SS/MG30L–10P/SS and Li/ MG30L–10P /Li have been prepared. The results of dc polarization measurements on the SS/MG30L–10P/SS and Li/ MG30L–10P /Li are carried out by applying a 30 mV dc bias voltage at 298 K as shown in Figures 6.31 and 6.32, respectively.

For the SS/MG30L–10P/SS cell, the value of the ionic transference number (t_{ion}) is 0.94. This is suggests that charge transport in these polymer electrolyte films is

predominantly due to ions; only a negligible contribution comes from electrons. Therefore, the lithium transfer number (t_{Li^+}) is 0.30.

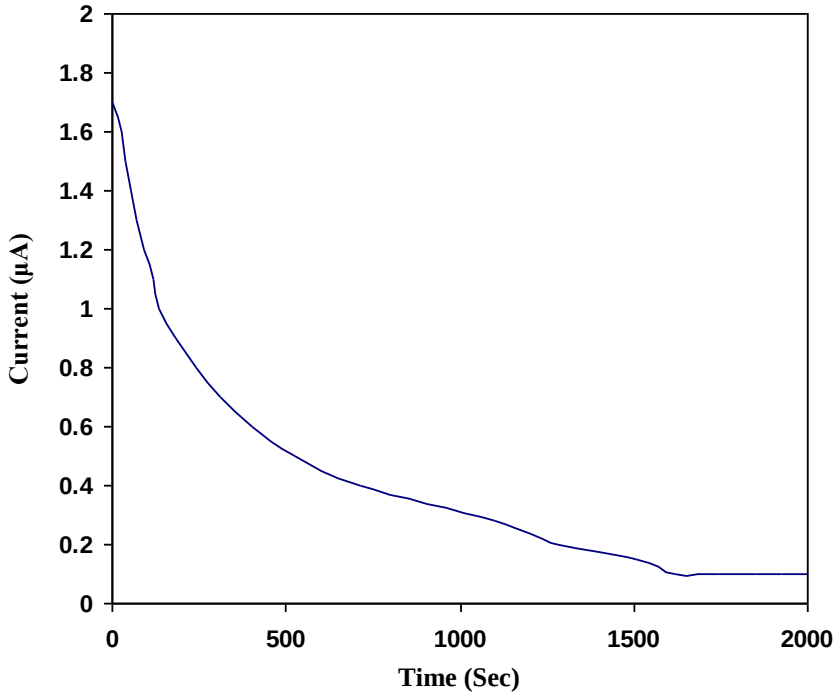

Figure 6.31 The polarization graph obtained using the SS/MG10L–10P/SS cell at 298 K

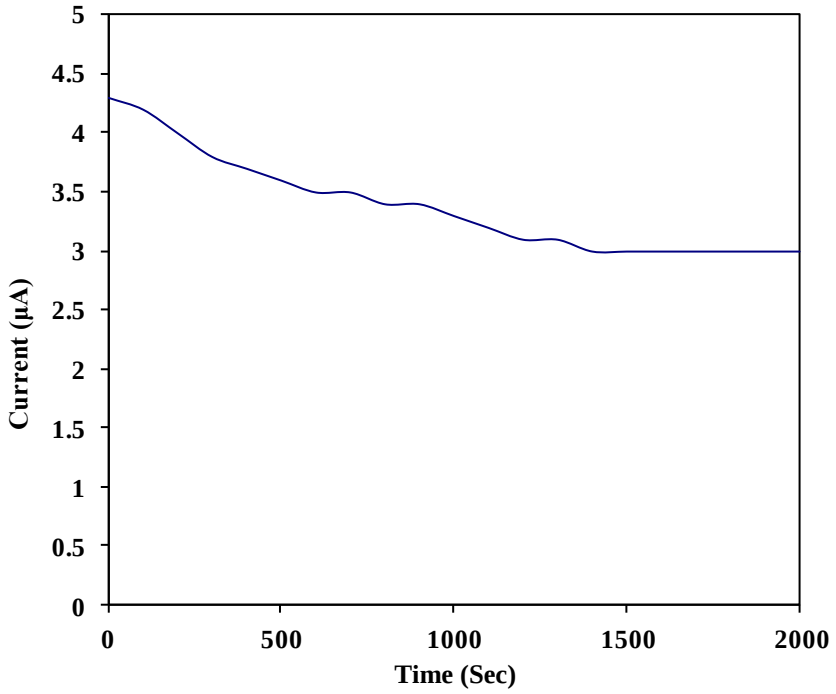

Figure 6.32 The polarization graph obtained using the Li/MG30L–10P/Li cell at 298 K

Summary

Conductivity for single–salt MG30–$LiCF_3SO_3$ system has increased from 1.69 × 10^{-6} S cm^{-1} to 1.46 x 10^{-5} S cm^{-1} in the double–salt MG30–$LiCF_3SO_3$–$LiN(CF_3SO_2)_2$ system and to 3.65 x 10^{-4} S cm^{-1} in the plasticized MG30–$LiCF_3SO_3$–PEG200 system. The double–salt and plasticized polymer electrolyte systems showed significant improvement in ionic conductivity as compared to single–salted MG30–$LiCF_3SO_3$ system.